Table 2. Summary of unreported mutations and deletions.

Patient ID	Age at onset	Clinical diagnosis	Enzyme assay (organ)	mtDNA variation	Locus	Heteroplasmy
377	1 year	LD	1 (Fb)	m.14439G>A	*ND6*	Homo (Fb)
190	1 year 6 months	LD	1,4 (M)	m.11246G>A	*ND4*	73% (fb)
508	0 days	SIDS	1 (Hep,Car)	m.4638A>G	*ND2*	86% (Fb), 0% (Hep, Car)
004	0 months	MC	1 (Fb)	m.5537A>G[1]	*tRNATrp*	27.4% (Fb)
271	0 months	ELBW	1 (Hep)	m.10045T>C	*tRNAGly*	Homo (hep)
312[2]	5 years	LD	1 (Fb) probably	m.1356A>G	*12S rRNA*	66% (Fb)
372	2 days	LIMD	1 (Hep)	Deletion (3424 bp) nt12493-15916		65.7% (Fb), 89.9% (Hep)
336	11 months	HD	1 (Hep)	Deletion (6639 bp) nt7734-14372		9.2% (Fb), 92.6% (Hep)
390	0 days	MC	1,4 (M,Hep)	Deletion (5424 bp) nt8574-13997		44.9% (Fb), 86.4% (Hep)

LIMD, lethal infantile mitochondrial disorder; HD, hepatic disease; LD, Leigh's disease; MC, mitochondrial cytopathy; SIDS, sudden infant death syndrome; ELBW, extremely low birth weight infant; Fb, fibroblast; Hep, liver; Car, heart; M, muscle.
[1]Expected to be causative because of the other reported mutation on the same position.
[2]m.1356A>G was confirmed as non-pathogenic and nDNA mutation was identified in Pt312.

showed bilateral and symmetrical hyperintensity foci in the basal ganglia. She developed progressive motor regression and became bedridden. Pt312 is a 5-year-old boy born after 36 weeks' gestation following a normal pregnancy to non-consanguineous parents. His birth weight was 2154 g. He has a sister who is his fraternal twin. At 5 months of age, his parents noticed hypotonia and nystagmus. At 10 months of age, he had generalized epilepsy and blood lactate and his pyruvate levels were high. A brain MRI revealed symmetrical high T2 signals in the midbrain.

Whole mtDNA sequencing and detection of variants

Genomic DNA (gDNA) was extracted from skin fibroblasts (Data S1), blood, liver, and cardiac muscle using either phenol/chloroform- or column-based extraction. Whole mtDNA was first polymerase chain reaction (PCR)-amplified as two separate large amplicons (LA1 and LA2) avoiding the nonspecific amplifications from nDNA.[9] Second-round PCR was performed using 46 primer pairs (mitoSEQrTM; Applied Biosystems, Carlsbad, CA) and the LA1 and LA2 amplicon mixture from first-round PCR as a template. PCR conditions were as follows: first-round PCR was performed in a reaction mixture containing 0.2 mmol/L of each dNTP, 0.25 U of Takara Ex Taq (Takara Bio, Shiga, Japan), 1× Ex Taq Buffer, 0.3 μmol/L of each primer, and extracted gDNA in a total volume of 50 μL. Initial denaturation was performed at 94°C for 2 min, followed by 30 cycles of 94°C for 20 sec, 60°C for 20 sec, and 72°C for 5 min, with a final extension at 72°C for 11 min. Second-round PCR was performed in a reaction mixture as above except with a 10,000-fold dilution of LA1 amplicon and a 100-fold dilution of LA2 amplicon (total volume of the PCR reaction, 10 μL). Initial denaturation was performed at 96°C for 5 min, followed by 30 cycles of 94°C for 30 sec, 60°C for 45 sec, and 72°C for 45 sec, with a final extension at 72°C for 10 min.

First- and second-round PCR products were separated by 1% and 2% agarose gels, respectively, then 10 μL of second-round PCR products were incubated with 1 μL of ExoSAP-IT reagent (GE Healthcare UK Ltd., Bucks, U.K.) at 37°C for 30 min to degrade remaining primers and nucleotides. The ExoSAP-IT reagent was then inactivated by incubating at 75°C for 15 min. PCR products were sequenced using a BigDye Terminator v3.1 cycle sequencing kit (Applied Biosystems) and an ABI3130xl Genetic Analyzer (Applied Biosystems). Sequence data were compared with the revised Cambridge sequence (GenBank Accession No. NC_012920.1) and sequences present in MITOMAP (http://mitomap.org/MITOMAP) and mtSNP (http://mtsnp.tmig.or.jp/mtsnp/index_e.shtml) using SeqScape software (Applied Biosystems). Whole mtDNA sequencing of seven samples was obtained using an Ion PGM™ sequencer (Life Technologies Corporation, Carlsbad, CA).

Characterization of mtDNA deletions

We searched for mtDNA deletions by focusing on the size of first-round PCR products in agarose electrophoresis. If PCR products were smaller than controls, we suspected mtDNA deletion and performed further analysis. The smaller PCR products were recovered from the gel and amplified by second-round PCR, as described above, and

© 2014 The Authors. *Annals of Clinical and Translational Neurology* published by Wiley Periodicals, Inc on behalf of American Neurological Association.

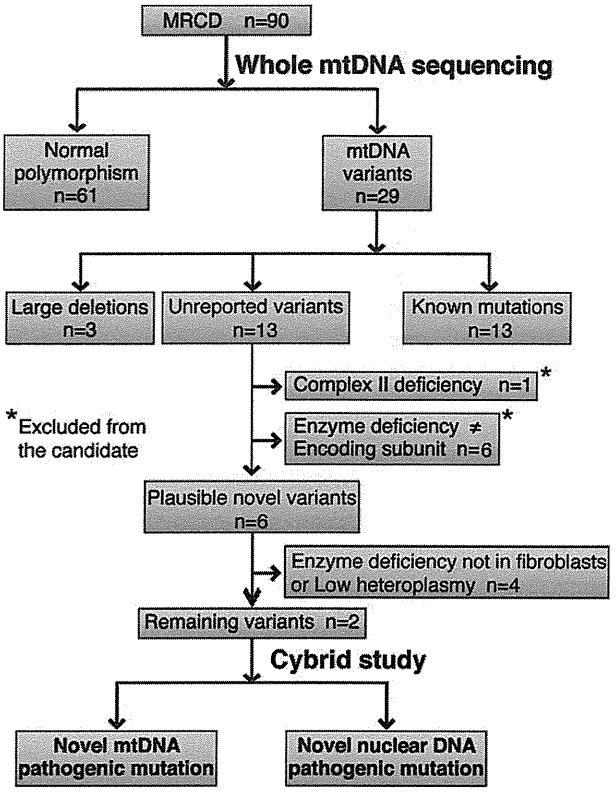

Figure 1. Flow diagram of study analysis. Ninety MRCD patients were analyzed in this study. Sixty-one patients had normal polymorphisms and 29 had mtDNA variants. Of these variants, 13 patients had MRCD causative mutations that had been previously described. We identified three novel large deletions and 13 unreported variants. Of the unreported variants, one patient with complex II deficiency was excluded because complex II is not encoded by mtDNA. Six patients were excluded because their enzyme deficiency pattern did not coincide with the variants found in mtDNA. Four patients were excluded because of the lack of fibroblast enzyme deficiency or low heteroplasmy. The remaining two cases were analyzed by cybrid study.

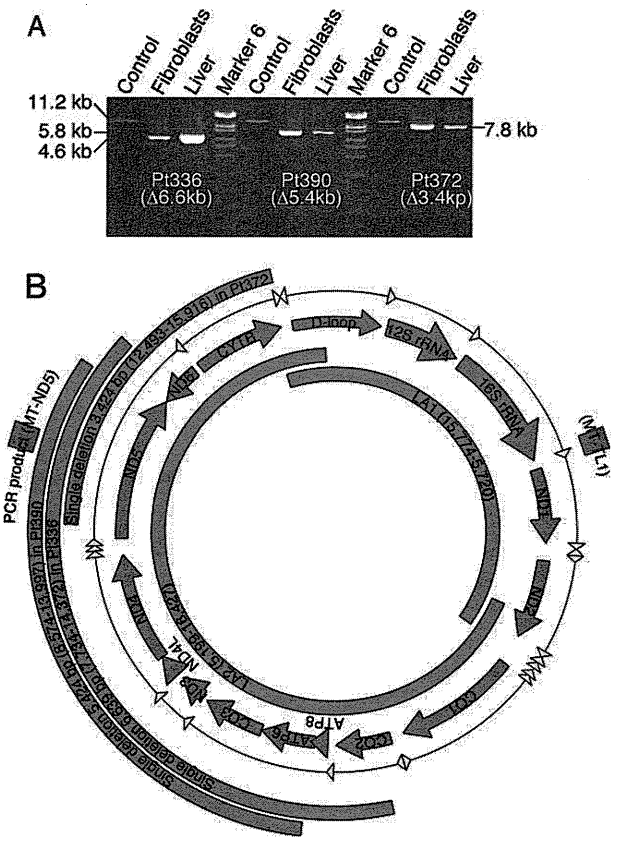

Figure 2. Identification of three large deletions. (A) Characterization of the three novel mtDNA deletions using agarose electrophoresis. First-round PCR products amplified from patient fibroblast and liver DNA clearly showed the presence of mtDNA deletions in Pt336, 390, and 372. Normal mtDNA from an MRCD patient was used as a positive control. (B) Positions of the novel mtDNA deletions are shown in blue. LA1 and LA2 amplification is shown in green. Two red squares represent real-time PCR amplicons MT-ND5 and MT-TL1.

analyzed for an mtDNA deletion. Second-round PCR was performed using fewer (25–26) PCR cycles to avoid untargeted DNA amplification. To identify the location of the deletion, we first compared the density of bands and screened the faint bands with agarose electrophoresis. The precise deletion boundaries were confirmed by sequencing analysis with primers used for second-round PCR that were close to the probable deletion region.

Results

Patient characteristics and their mtDNA mutations

A total of 90 patients (49 were men and 41 were women) with MRCD were subjected to whole mtDNA sequencing analysis (Table 1). Eighty-four subjects (93%) were non-consanguineous. Seventy-six subjects (84%) were aged 1 year or younger. We identified 13 previously reported mtDNA mutations, 13 unreported variants, and three novel deletions (Fig. 1). The remaining 61 subjects had normal polymorphisms in their mtDNA (Fig. 1).

Large mtDNA deletions were identified in three patients

Agarose gel electrophoresis of first-round PCR from fibroblast and liver mtDNA clearly showed the presence of mtDNA deletions in Pt336, 390, and 372 (Fig. 2A). The precise deletion sites were confirmed by sequencing analysis. The expected size of the first-round PCR LA2 product in wild-type mtDNA from an MRCD patient was 11.2 kb, which enabled us to estimate the deletion sizes

 © 2014 The Authors. *Annals of Clinical and Translational Neurology* published by Wiley Periodicals, Inc on behalf of American Neurological Association.

of Pt336, 390, and 372 as 6639, 5424, and 3424 bp, respectively (Fig. 2A and B). In Pt336, the 6639-bp deletion was located between nucleotides 7734 and 14,372 and was flanked by 5-bp perfect direct repeats. This deletion results in the loss of 15 genes (*CO2, ATP8, ATP6, CO3, ND3, ND4L, ND4, ND5, ND6,* and six *tRNA* genes). The heteroplasmy ratio of this deletion was 9.2% in the fibroblasts (Fb) and 92.6% in the liver (Hep) (Table 2 and Data S1). In Pt390, the 5424-bp deletion was located between nucleotide positions 8574 and 13,997 and was flanked by 11-bp imperfect direct repeats. This deletion results in the loss of 11 genes (*ATP6, CO3, ND3, ND4L, ND4, ND5,* and five *tRNA* genes). The heteroplasmy ratio of this deletion was 44.9% (Fb) and 86.4% (Hep) (Table 2). In Pt372, the 3424-bp deletion was located between nucleotides 12,493 and 15,916 and was flanked by 6-bp imperfect direct repeats. This deletion results in the loss of five genes (*ND5, ND6, CYB,* and two *tRNA* genes). The heteroplasmy ratio of this deletion was 65.7% (Fb), and 89.9% (Hep) (Table 2).

Unreported variants of mtDNA detected in 13 patients

We identified 13 unreported mtDNA variants. Of these, seven were excluded by manual curation (Fig. 1). One of these was excluded because the enzyme deficiency was specific to complex II, which is not encoded by mtDNA. The other six were excluded because their enzyme deficiency pattern did not coincide with the variants found in mtDNA. From the remaining six plausible mtDNA variants, we determined whether they were causative using the following inclusion criteria for further analysis: (1) cells were viable for further assay, (2) mtDNA variants corresponded to the enzyme assay data in the RC subunit, (3) enzyme deficiency was observed in the fibroblasts, and (4) variants had high heteroplasmy ratios (Fig. 1 and Table 2). On the basis of these criteria, we selected two patients whose mtDNA variants (m.14439G>A in *MT-ND6* and m.1356A>G in *12S rRNA*) were suitable for further analysis as shown in Figure 1. The other four patients were excluded because they did not show enzyme deficiency in their fibroblasts or because of low heteroplasmy ratios (Table 2).

m.14439G>A (*MT-ND6*), but not m.1356A>G (12S rRNA), is a causative mutation

The m.14439G>A (*MT-ND6*) variant was observed in fibroblasts from Pt377 (Fig. 3A). PCR- restriction fragment length polymorphism (RFLP) analysis with the *Hpy*188I restriction enzyme found Pt377 fibroblasts to be homoplasmic, and the m.14439G>A variant was not detected in the blood of the patient's parents (Fig. 3A and B). This mutation changes the proline to a serine at amino acid position 79, which is highly conserved among vertebrates (Fig. 3C). ND6 is one of the mtDNA-encoded complex I subunits and alignment of the ND6 protein in different species revealed conservation of amino acids. The activity level of the RC complex I was coincidentally reduced in the patient's fibroblasts (Fig. 4A). To further confirm whether this mutation was causative of mitochondrial dysfunction, we performed cybrid analysis (Data S1). The cybrids showed a reduction in the complex I activity level consistent with the respiratory enzyme assay in the patient's fibroblasts (Fig. 4B). These data strongly support the idea that the m.14439G>A *(ND6)* mutation detected in Pt377 is responsible for the complex I deficiency.

The m.1356A>G (*12S rRNA*) variant was observed in fibroblasts from Pt312, which showed reduced activity levels of RC complex I (Fig. 4A). By mismatch PCR-RFLP-analysis using the *Sty*I restriction enzyme, this variant was determined at a heteroplasmy ratio of 66% in the patient's fibroblasts (Table 2). The cybrids harboring this variant showed a recovery of complex I enzyme activity compared with the original patient's fibroblasts (Fig. 4B). These data suggest that reduced complex I enzyme activity was rescued by nuclear DNA and that this mtDNA variation is not causative. This further indicates that the nuclear gene mutation is the cause of MRCD in this patient.

Identification of the c.55C>T (*NDUFA1*) mutation in Pt312 by whole exome sequencing

To search for the causative nuclear gene mutation in Pt312, we performed whole exome sequencing (Data S1). This identified a single hemizygous mutation (c.55C>T) in exon 1 of the *NDUFA1* gene, which altered the amino acid residue at position 19 from proline to serine (p. P19S). The mutation was confirmed by Sanger sequencing (Fig. 5A). This conserved proline residue lies within the hydrophobic N-terminal side constituting a functional domain that is involved in mitochondrial targeting, import, and orientation of *NDUFA1*.[10,11] SIFT and PolyPhen, which predict the function of non-synonymous variants (http://genetics.bwh.harvard.edu/pph/), also revealed that the p.P19S mutation "probably" damages the function of the NDUFA1 protein (damaging score, 0.956). Alignment of the NDUFA1 protein between different species revealed the conservation of three amino acids, including the proline at position 19, which is highly conserved among vertebrates (Fig. 5B). To further confirm if the complex I deficiency in Pt312 occurred because of the mutation in *NDUFA1*, we overexpressed *NDUFA1* cDNA to determine if the enzyme deficiency

© 2014 The Authors. *Annals of Clinical and Translational Neurology* published by Wiley Periodicals, Inc on behalf of American Neurological Association.

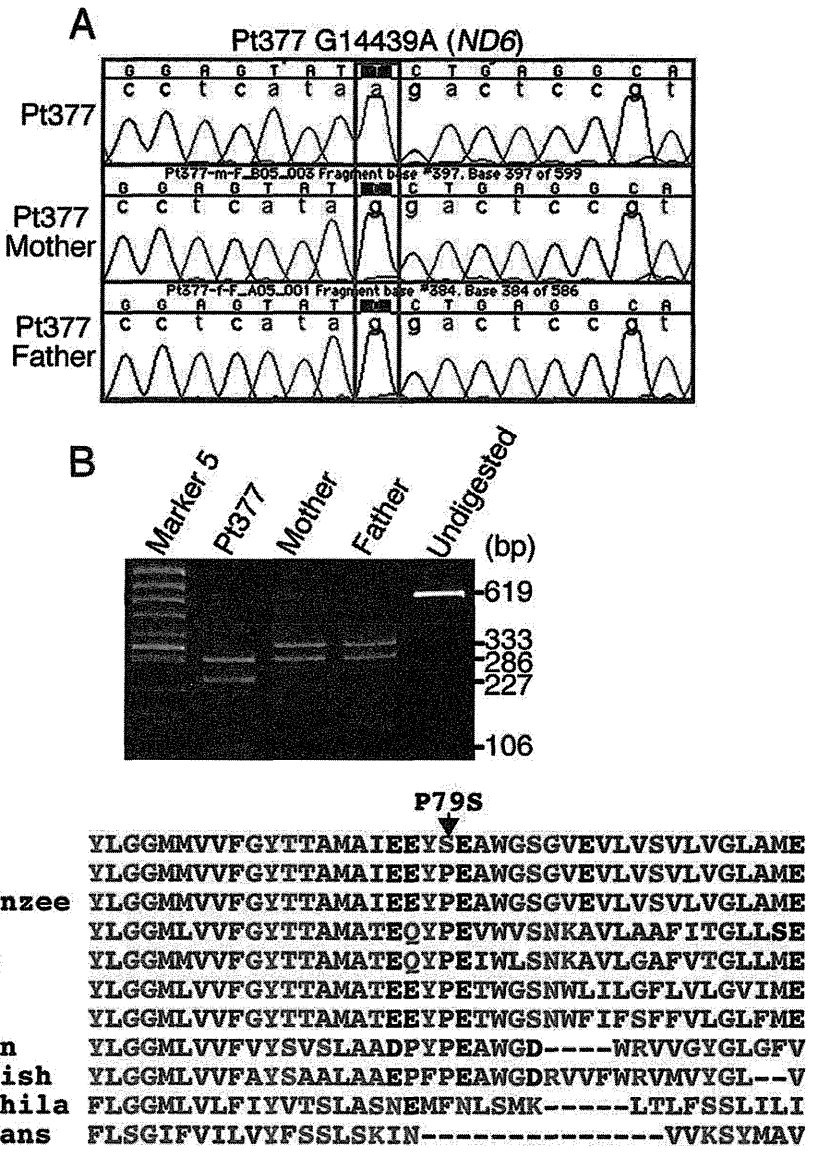

Figure 3. Novel mutation m.14439G>A in Pt377 mtDNA. (A) Trio-sequencing analysis of m.14439G>A (*MT-ND6* p.P79S) change in Pt377 family. Sequence chromatograms show that the m.14439G>A is detectable only in Pt377. (B) PCR-RFLPanalysis using fibroblast mtDNA from Pt377 and blood from both parents. A 619-bp PCR fragment was digested with *Hpy*188I. Wild-type mtDNA was cleaved into two fragments of 333 and 286 bp as shown in "Mother" and "Father", whereas the PCR product containing the m.14439G>A mutation was cleaved into three fragments: 286, 227, and 106 bp ("Pt377"). Undigested = undigested PCR product. (C) Alignment of MT-ND6 protein between different species shows the conservation of amino acid Proline 79. Amino acid sequences of *MT-ND6* gene products were aligned by ClustalW program (http://www.ebi.ac.uk/Tools/msa/clustalw2/) and NCBI/homologene (http://www.ncbi.nlm.nih.gov/homologene).

could be recovered (Data S1). Lentiviral transfection of NDUFA1 resulted in a significant increase in complex I assembly level as determined by blue native polyacrylamide gel electrophoresis. By contrast, lentiviral transfection of control mtTurboRFP did not rescue the phenotype (Fig. 5C). These data indicate that the c.55C>T mutation in *NDUFA1* is responsible for the complex I deficiency in Pt312.

Discussion

MRCD is particularly difficult to diagnose in pediatric cases as the clinical features are highly variable. We, therefore, propose a systematic approach for diagnosing MRCD that starts with a biochemical enzyme assay and is followed by whole mtDNA sequencing. In this study, we performed whole mtDNA sequencing for 90 children with

 © 2014 The Authors. *Annals of Clinical and Translational Neurology* published by Wiley Periodicals, Inc on behalf of American Neurological Association.

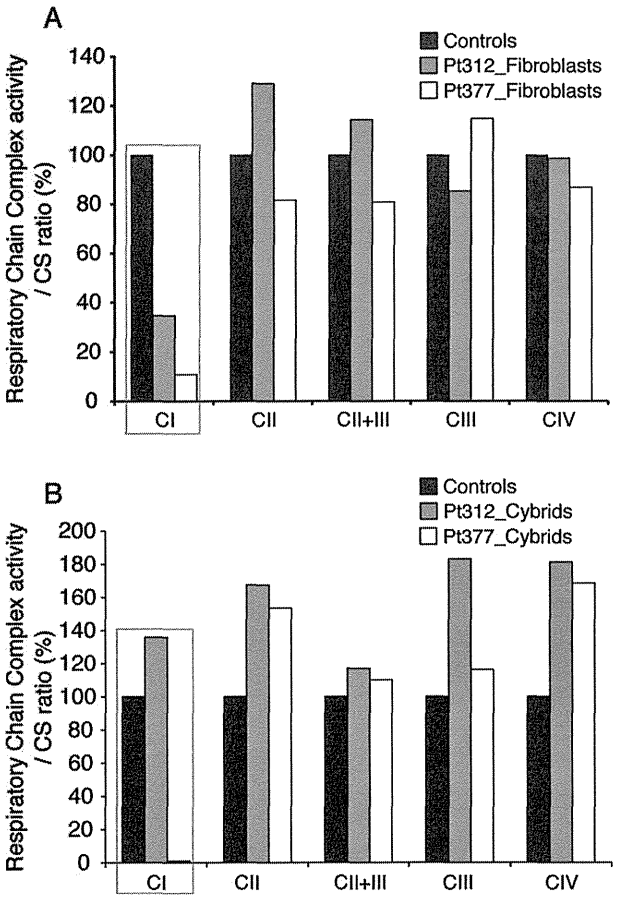

Figure 4. Biochemical assay for respiratory chain enzyme activity in fibroblasts and cybrid cells from Pt377 and Pt312. (A) Respiratory chain complex enzyme activity for CI, CII, CII + III, and CIV in skin fibroblast mitochondria from Pt312 and Pt377 compared with normal controls. The activity of each complex was calculated as a ratio relative to citrate synthase (CS). CI showed a reduction in enzyme activity in Pt312 and 377 fibroblasts. (B) Respiratory chain complex enzyme activity of cybrids established from Pt312 and Pt377 fibroblasts. Cybrids were established from rho0-HeLa cell and Pt312 or Pt377 fibroblasts. The activity of each complex in these cybrids was calculated as a ratio relative to that of citrate synthase (CS).

MRCD, and identified 29 mtDNA variants. Of these, we identified 13 known causative mutations, three large deletions, and further confirmed that m.14439G>A (*MT-ND6*) and c.55C>T (*NDUFA1*) are new causative mutations for MRCD from the results of a cybrid assay, whole exome sequencing, and a complementation study. The diagnosis of MRCD was then confirmed as definite by molecular analysis in these 18 cases.

Whole mitochondrial DNA sequencing identified 13 cases (14%) harboring known causative mtDNA mutations. mt. 10191T>C (*ND3*) and mt. 8993T>C or G (*ATP6*) mutations were detected in three and two patients, respectively (data not shown). Both are common causative mutations of infantile Leigh syndrome. Previous reports found that most common MRCD causative mutations are primarily responsible for adult-onset disease, whereas few are responsible for childhood-onset MRCD;[12,13] only 14% of our cases were attributed to known mtDNA mutations.

Most patients in this study were 1-year old or younger at the onset of disease, with no family history. We used the RC complex enzyme assay to diagnose pediatric patients who had not been diagnosed with MRCD in a clinical setting. Several MRCD cases in children were previously reported to be difficult to diagnose with nonspecific clinical presentations in contrast to the characteristic clinical syndromes such as MELAS and MERRF caused by common mtDNA mutations.[6,12]

We identified three novel deletions that we concluded were causative because they include several genes that could explain the deficiency of the RC enzymes. Generally, most mtDNA deletions share similar structural characteristics, are located in the major arc between two proposed origins of replication (OH and OL; Mitomap), and are predominantly (~85%) flanked by short direct repeats.[14,15] Single mtDNA deletions are reported to be the common causes of sporadic MRCD such as Kearns-Sayre syndrome (KSS), CPEO, and Pearson's syndrome. In this study, all three deletions were located in the major arc and were flanked by repeat sequences, similar to previous studies. Although Pt390 was diagnosed with Pearson's syndrome, the other two patients (Pt336 and Pt372) did not show a common phenotype caused by a single deletion such as KSS, CPEO, or Pearson's syndrome. Therefore, screening by mtDNA size differences is important even in those patients not clinically suspected to have mtDNA deletions.

Manual curation identified six plausible mtDNA variants that had not previously been reported (Fig. 1). We attempted to carry out a functional assay of the two patients whose fibroblasts are enzyme deficient, although it was difficult to apply this strategy to those fibroblasts with normal enzyme activity. In this sense, it is important to collect patients with similar phenotypes and carrying the same mtDNA variants to accurately diagnose the causal mutation. Thus, this study of patients harboring unreported mtDNA variants will be useful in a clinical situation. Of these, the m.14439G>A (*MT-ND6*) variant was experimentally confirmed to be a novel causative mtDNA mutation, while 1356A>G (*12S rRNA*) was confirmed to be non-pathogenic by a cybrid assay. The remaining four novel variants have yet to be experimentally elucidated, but m.5537A>G (*mt-tRNA trp*) in Pt004 is likely to be causative because m.5537AinsT was reported to be disease causing.[16]

ND6 is an mtDNA-encoded complex I subunit that is essential for the assembly of complex I and the maintenance of its structure.[17–19] *ND6* mutations were previ-

© 2014 The Authors. *Annals of Clinical and Translational Neurology* published by Wiley Periodicals, Inc on behalf of American Neurological Association.

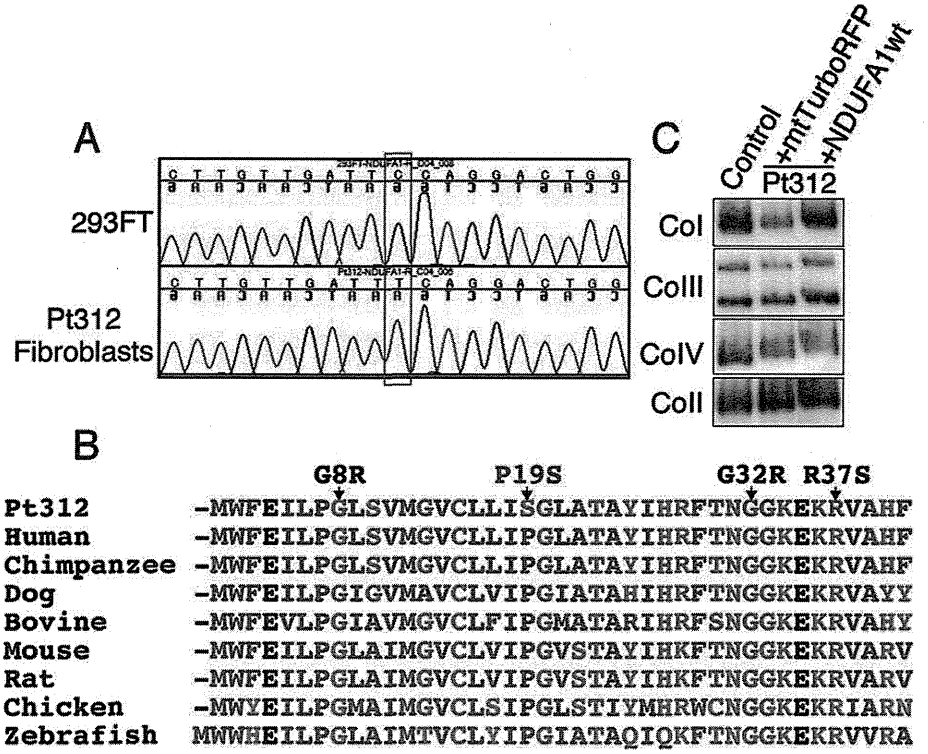

Figure 5. The novel nDNA mutation c.55C>T in *NDUFA1*. (A) Sequence chromatograms showing the c.55C>T (*NDUFA1* p.P19S) mutation in Pt312 and 293FT genomic DNA as a wild-type control. (B) Alignment of amino acid sequences of NDUFA1 subunit between different species shows the high conservation of amino acid Proline 19. G8R, G32R, and R37S show reported pathogenic mutations in *NDUFA1*. (C) Blue native polyacrylamide gel electrophoresis for CI, CII, CIII, and CIV following lentiviral transductions. Transduction of wild-type *NDUFA1* cDNA into Pt312 fibroblasts using recombinant lentivirus rescued complex I assembly levels of the fibroblasts, similar to the transduction of mtTurboRFP into normal fibroblasts (fHDF). As control gene of candidate genes, mtTurboRFP was used which inserted mitochondrial targeting signal sequence to N terminal of TurboRFP protein. By contrast, lentiviral transduction of control mtTurboRFP into Pt312 fibroblasts decreased the assembly level of complex I.

ously found to be associated with Leigh syndrome[20] and MELAS,[21] and this gene region is also reported to be a hot spot for LHON mutations.[22] Mitochondrial *12S rRNA* is a hot spot for mutations associated with aminoglycoside ototoxicity and non syndromic hearing loss, although mutations in this gene have not been reported to cause syndromic mitochondrial disorders.[23] We found that the m.14439G>A mutation altered an evolutionarily conserved proline to a serine in the hydrophilic inner membrane space of the ND6 protein[22] (Fig. 3C). As this mutation was homoplasmic in the patient's fibroblasts and absent from the blood of unaffected parents (Fig. 3A and B), this suggests that it developed de novo.

Exome sequencing in this study identified a single hemizygous change (c.55C>T, p.P19S) in exon 1 of the X-linked *NDUFA1* gene. To date, three missense mutations (G8R,[10] G32R,[24] and R37S[10]) have been reported in *NDUFA1* that are associated with neurological symptoms. *NDUFA1* was shown to interact with the subunits encoded by mtDNA during the complex I assembly process.[11]

Cybrid study is a powerful tool for detecting pathogenicity of either mtDNA or nDNA origin, although patients' cells showing RC enzyme deficiency are inevitable. Nevertheless, a major limitation of this technique is the length of time to establish transmitochondrial cybrids. We would, therefore, propose a systematic approach for diagnosing MRCD that starts with a biochemical enzyme assay and is followed by whole mtDNA sequencing. For patients with no apparent putative mtDNA mutations, whole exome sequencing is a powerful tool to diagnose nuclear gene mutations especially in cases when molecular diagnosis leads to appropriate genetic counseling.

Acknowledgments

We thank T. Hirata and Y. Yatsuka for their technical assistance. This study was supported in part by a grant from the Research Program of Innovative Cell Biology by Innovative Technology (Cell Innovation), a Grant-in-Aid for the Development of New Technology from The Promotion and Mutual Aid Corporation for Private

 © 2014 The Authors. *Annals of Clinical and Translational Neurology* published by Wiley Periodicals, Inc on behalf of American Neurological Association.

Schools of Japan from MEXT (to Y. O.), a Grant-in-Aid research grants for Scientific Research (A-22240072, B-21390459, A-25242062) from the Ministry of Education, Culture, Sports, Science, and Technology (MEXT) of Japan to M. T., and a Grant-in-Aids (H23-016, H23-119, and H24-005) for the Research on Intractable Diseases (Mitochondrial Disease) from the Ministry of Health, Labour and Welfare (MHLW) of Japan to M. T. and A. O., and a Grant-in-Aids (H23-001, H24-017, H24-071) for the Research on Intractable Diseases from the Ministry of Health, Labour and Welfare (MHLW) of Japan to A. O.

Conflict of Interest

None declared.

References

1. Calvo S, Jain M, Xie X, et al. Systematic identification of human mitochondrial disease genes through integrative genomics. Nat Genet 2006;38:576–582.
2. Zeviani M, Di Donato S. Mitochondrial disorders. Brain 2004;127(Pt 10):2153–2172.
3. Munnich A, Rötig A, Chretien D, et al. Clinical presentation of mitochondrial disorders in childhood. J Inherit Metab Dis 1996;19:521–527.
4. Skladal D, Halliday J, Thorburn DR. Minimum birth prevalence of mitochondrial respiratory chain disorders in children. Brain 2003;126(Pt 8):1905–1912.
5. Kisler JE, Whittaker RG, McFarland R. Mitochondrial diseases in childhood: a clinical approach to investigation and management. Dev Med Child Neurol 2010;52: 422–433.
6. Thorburn DR. Mitochondrial disorders: prevalence, myths and advances. J Inherit Metab Dis 2004;27:349–362.
7. Zeviani M, Bertagnolio B, Uziel G. Neurological presentations of mitochondrial diseases. J Inherit Metab Dis 1996;19:504–520.
8. Bernier FP, Boneh A, Dennett X, et al. Diagnostic criteria for respiratory chain disorders in adults and children. Neurology 2002;59:1406–1411.
9. Akanuma J, Muraki K, Komaki H, et al. Two pathogenic point mutations exist in the authentic mitochondrial genome, not in the nuclear pseudogene. J Hum Genet 2000;45:337–341.
10. Potluri P, Davila A, Ruiz-Pesini E, et al. A novel NDUFA1 mutation leads to a progressive mitochondrial complex I-specific neurodegenerative disease. Mol Genet Metab 2009;96:189–195.
11. Yadava N, Houchens T, Potluri P, Scheffler IE. Development and characterization of a conditional mitochondrial complex I assembly system. J Biol Chem 2004;279:12406–12413.
12. Elliott HR, Samuels DC, Eden JA, et al. Pathogenic mitochondrial DNA mutations are common in the general population. Am J Hum Genet 2008;83:254–260.
13. Shoffner JM. Oxidative phosphorylation disease diagnosis. Ann N Y Acad Sci 1999;893:42–60.
14. Bua E, Johnson J, Herbst A, et al. Mitochondrial DNA-deletion mutations accumulate intracellularly to detrimental levels in aged human skeletal muscle fibers. Am J Hum Genet 2006;79:469–480.
15. Krishnan KJ, Reeve AK, Samuels DC, et al. What causes mitochondrial DNA deletions in human cells? Nat Genet 2008;40:275–279.
16. Tulinius M, Moslemi AR, Darin N, et al. Leigh syndrome with cytochrome-c oxidase deficiency and a single T insertion nt 5537 in the mitochondrial tRNATrp gene. Neuropediatrics 2003;34:87–91.
17. Bai Y, Attardi G. The mtDNA-encoded ND6 subunit of mitochondrial NADH dehydrogenase is essential for the assembly of the membrane arm and the respiratory function of the enzyme. EMBO J 1998;17:4848–4858.
18. Cardol P, Matagne RF, Remacle C. Impact of mutations affecting ND mitochondria-encoded subunits on the activity and assembly of complex I in Chlamydomonas. Implication for the structural organization of the enzyme. J Mol Biol 2002;319:1211–1221.
19. Ugalde C, Triepels RH, Coenen MJ, et al. Impaired complex I assembly in a Leigh syndrome patient with a novel missense mutation in the ND6 gene. Ann Neurol 2003;54:665–669.
20. Kirby DM, Kahler SG, Freckmann ML, et al. Leigh disease caused by the mitochondrial DNA G14459A mutation in unrelated families. Ann Neurol 2000;48:102–104.
21. Ravn K, Wibrand F, Hansen FJ, et al. An mtDNA mutation, 14453G–>A, in the NADH dehydrogenase subunit 6 associated with severe MELAS syndrome. Eur J Hum Genet 2001;9:805–809.
22. Chinnery PF, Brown DT, Andrews RM, et al. The mitochondrial ND6 gene is a hot spot for mutations that cause Leber's hereditary optic neuropathy. Brain 2001;124 (Pt 1):209–218.
23. Prezant TR, Agapian JV, Bohlman MC, et al. Mitochondrial ribosomal RNA mutation associated with both antibiotic-induced and non-syndromic deafness. Nat Genet 1993;4:289–294.
24. Fernandez-Moreira D, Ugalde C, Smeets R, et al. X-linked NDUFA1 gene mutations associated with mitochondrial encephalomyopathy. Ann Neurol 2007;61:73–83.

Supporting Information

Additional Supporting Information may be found in the online version of this article:

Data S1. Supplementary methods.

© 2014 The Authors. *Annals of Clinical and Translational Neurology* published by Wiley Periodicals, Inc on behalf of American Neurological Association.

REPORT

Mutations in *GTPBP3* Cause a Mitochondrial Translation Defect Associated with Hypertrophic Cardiomyopathy, Lactic Acidosis, and Encephalopathy

Robert Kopajtich,[1,31] Thomas J. Nicholls,[2,31] Joanna Rorbach,[2,31] Metodi D. Metodiev,[3,31] Peter Freisinger,[4] Hanna Mandel,[5] Arnaud Vanlander,[6] Daniele Ghezzi,[7] Rosalba Carrozzo,[8] Robert W. Taylor,[9] Klaus Marquard,[10] Kei Murayama,[11] Thomas Wieland,[1,12] Thomas Schwarzmayr,[1,12] Johannes A. Mayr,[13] Sarah F. Pearce,[2] Christopher A. Powell,[2] Ann Saada,[14] Akira Ohtake,[15] Federica Invernizzi,[7] Eleonora Lamantea,[7] Ewen W. Sommerville,[9] Angela Pyle,[16] Patrick F. Chinnery,[16] Ellen Crushell,[17] Yasushi Okazaki,[18,19] Masakazu Kohda,[18] Yoshihito Kishita,[19] Yoshimi Tokuzawa,[19] Zahra Assouline,[20] Marlène Rio,[20] François Feillet,[21] Bénédict Mousson de Camaret,[22] Dominique Chretien,[3] Arnold Munnich,[3,20] Björn Menten,[23] Tom Sante,[23] Joél Smet,[6] Luc Régal,[24] Abraham Lorber,[25] Asaad Khoury,[25] Massimo Zeviani,[2,7] Tim M. Strom,[1,12] Thomas Meitinger,[1,12,26,27,28] Enrico S. Bertini,[8] Rudy Van Coster,[6] Thomas Klopstock,[28,29,30] Agnès Rötig,[3] Tobias B. Haack,[1,12] Michal Minczuk,[2,*] and Holger Prokisch[1,12,*]

Respiratory chain deficiencies exhibit a wide variety of clinical phenotypes resulting from defective mitochondrial energy production through oxidative phosphorylation. These defects can be caused by either mutations in the mtDNA or mutations in nuclear genes coding for mitochondrial proteins. The underlying pathomechanisms can affect numerous pathways involved in mitochondrial physiology. By whole-exome and candidate gene sequencing, we identified 11 individuals from 9 families carrying compound heterozygous or homozygous mutations in *GTPBP3*, encoding the mitochondrial GTP-binding protein 3. Affected individuals from eight out of nine families presented with combined respiratory chain complex deficiencies in skeletal muscle. Mutations in *GTPBP3* are associated with a severe mitochondrial translation defect, consistent with the predicted function of the protein in catalyzing the formation of 5-taurinomethyluridine (τm^5U) in the anticodon wobble position of five mitochondrial tRNAs. All case subjects presented with lactic acidosis and nine developed hypertrophic cardiomyopathy. In contrast to individuals with mutations in *MTO1*, the protein product of which is predicted to participate in the generation of the same modification, most individuals with *GTPBP3* mutations developed neurological symptoms and MRI involvement of thalamus, putamen, and brainstem resembling Leigh syndrome. Our study of a mitochondrial translation disorder points toward the importance of posttranscriptional modification of mitochondrial tRNAs for proper mitochondrial function.

Defects of the mitochondrial respiratory chain underlie a diverse group of human disorders characterized by impaired oxidative phosphorylation (OXPHOS). The generation of a functional respiratory chain requires the coordinated expression of both the nuclear genome and mitochondrial DNA (mtDNA). Defective translation of mtDNA-encoded proteins, caused by mutations in either the mitochondrial or nuclear genomes, represents a rapidly expanding group of human disorders, which often manifest as severe infantile combined OXPHOS deficiencies.[1]

[1]Institute of Human Genetics, Helmholtz Zentrum München, German Research Center for Environmental Health, 85764 Neuherberg, Germany; [2]MRC Mitochondrial Biology Unit, Hills Road, Cambridge CB2 0XY, UK; [3]INSERM U1163, Université Paris Descartes-Sorbonne Paris Cité, Institut Imagine, 75015 Paris, France; [4]Department of Pediatrics, Klinikum Reutlingen, 72764 Reutlingen, Germany; [5]Metabolic Unit, Children's Hospital, Ramban Health Care Campus, 31096 Haifa, Israel; [6]Department of Pediatric Neurology and Metabolism, University Hospital Ghent, 9000 Ghent, Belgium; [7]Unit of Molecular Neurogenetics, Fondazione IRCCS (Istituto di Ricovero e Cura a CarattereScientifico) Istituto Neurologico "Carlo Besta," 20126 Milan, Italy; [8]Unità di Malattie Neuromuscolari e Neurodegenerative, Laboratorio di Medicina Molecolare, Dipartimento di Neuroscienze, IRCCS Ospedale Pediatrico Bambino Gesù, 00165 Roma, Italy; [9]Wellcome Trust Centre for Mitochondrial Research, Institute of Neuroscience, Newcastle University, Newcastle upon Tyne NE2 4HH, UK; [10]Department of Neuropediatrics, Klinikum Stuttgart, 70176 Stuttgart, Germany; [11]Department of Metabolism, Chiba Children's Hospital, Chiba 266-0007, Japan; [12]Institute of Human Genetics, Technische Universität München, 81675 Munich, Germany; [13]Department of Pediatrics, Paracelsus Medical University Salzburg, 5020 Salzburg, Austria; [14]Monique and Jacques Roboh Department of Genetic Research and the Department of Genetics and Metabolic Diseases, Hadassah-Hebrew University Medical Center, 91120 Jerusalem, Israel; [15]Department of Pediatrics, Faculty of Medicine, Saitama Medical University, Saitama 350-0495, Japan; [16]Wellcome Trust Centre for Mitochondrial Research, Institute of Genetic Medicine, Newcastle University, Newcastle upon Tyne NE1 3BZ, UK; [17]Metabolic Paediatrician, National Centre for Inherited Metabolic Disorders, Temple Street Children's University Hospital, Dublin 1, Ireland; [18]Department of Translational Research, Research Center for Genomic Medicine, Saitama Medical University, Saitama 350-1241, Japan; [19]Department of Functional Genomics & Systems Medicine, Research Center for Genomic Medicine, Saitama Medical University, Saitama 350-1241, Japan; [20]Departments of Pediatrics and Genetics, Hôpital Necker-Enfants Malades, 75015 Paris, France; [21]Service de médecine infantile, Hôpitald'Enfants de Brabois, CHU de Nancy, 54511 Vandoeuvre-les Nancy, France; [22]Service des Maladies Héréditaires du Métabolisme, CHU de Lyon, 69677 Bron, France; [23]Center for Medical Genetics, Ghent University, Ghent University Hospital, 9000 Ghent, Belgium; [24]Department of Pediatrics, Metabolic Center, University Hospital Leuven, 3000 Leuven, Belgium; [25]Department of Pediatric Cardiology, Ramban Medical Center, 31096 Haifa, Israel; [26]DZHK (German Centre for Cardiovascular Research), partner site Munich, 81675 Munich, Germany; [27]Munich Heart Alliance, 80802 Munich, Germany; [28]Munich Cluster for Systems Neurology (SyNergy), 80336 Munich, Germany; [29]German Research Center for Neurodegenerative Diseases (DZNE), 80336 Munich, Germany; [30]Department of Neurology, Friedrich-Baur-Institute, Ludwig-Maximilians-University, 80336 Munich, Germany
[31]These authors contributed equally to this work
*Correspondence: michal.minczuk@mrc-mbu.cam.ac.uk (M.M.), prokisch@helmholtz-muenchen.de (H.P.)
http://dx.doi.org/10.1016/j.ajhg.2014.10.017. ©2014 by The American Society of Human Genetics. All rights reserved.

The mitochondrial genome contains a total of 37 genes, 13 of which encode protein subunits of the respiratory chain complexes and the ATP synthase. Translation of these genes is achieved by the organelle's own protein synthesis machinery, of which only the RNA components (rRNAs and tRNAs) are encoded by mtDNA. All protein factors required for mitochondrial translation are encoded in the nucleus and must be imported after their synthesis in the cytoplasm. Mitochondrial (mt-) tRNAs require extensive posttranscriptional modifications before achieving translation competency. Modifications to tRNAs might contribute to their proper folding, stability, or decoding capacity. In mitochondria a minimal set of 22 different tRNAs is used to translate all codons.[2] Modifications to the wobble position of the anticodon loop of mt-tRNAs play an important role in ensuring correct mRNA-tRNA interactions. In ten mt-tRNA species, all of which correspond to two codon sets, four different types of modified nucleotides have been identified at the wobble position.[3,4] One of these modifications is 5-taurinomethyluridine (τm^5U), found at position 34 (U34) of mt-tRNAsLeu^{UUR}, Trp, Gln, Lys, and Glu, which has been suggested to be synthesized cooperatively by GTPBP3 and MTO1.[5] In addition to τm^5U, mt-tRNAs Gln, Lys, and Glu also contain a 2-thiouridine modification at U34 (s^2U), introduced by TRMU (also known as MTU1). This results in a 5-taurinomethyl-2-thiouridine ($\tau m^5 s^2 U$) modification in these mt-tRNA molecules. Modifications of U34 have been proposed to modulate either the accuracy or the efficiency of translation.[6,7] Three types of mutations affecting U34 have been associated with human mitochondrial disease: (1) mutations in the mt-tRNAs;[8] (2) mutations in *TRMU* (MIM 610230) affecting U34 2-thiouridylation and leading to acute infantile liver failure resulting from combined OXPHOS deficiency;[9] and (3) more recently, mutations in *MTO1* (MIM 614667) found to underlie cases of hypertrophic cardiomyopathy and lactic acidosis, associated with impaired mitochondrial translation rate and reduced respiratory chain activities.[10,11]

Whole-exome sequencing (WES) of 790 individuals with suspected mitochondriopathy in five centers identified eight index case subjects (plus two affected siblings) with homozygous or two heterozygous rare variants (minor allele frequency < 0.1%) in *GTPBP3* (MIM 608536), with no such case being found in 11,295 control subjects. This presents a genome-wide significant enrichment in *GTPBP3* (RefSeq accession number NM_032620.3) mutation load in samples from individuals with the clinical diagnosis "mitochondrial disease" ($p < 3.2 \times 10^{-10}$, Fisher exact test) in comparison to nonmitochondrial disorder samples. In addition, when filtering for genes coding for mitochondrial proteins,[12] in several individuals *GTPBP3* was the only gene with two mutations. Further evidence for the pathogenic role of *GTPBP3* mutations was derived from follow-up candidate gene sequencing of 18 individuals with similar phenotypes, which identified two more index cases. Collectively, mutations in *GTPBP3* were detected in 12 individuals from 10 families. However, segregation analysis of a single affected individual (#66654) revealed that the two identified heterozygous mutations in *GTPBP3* affected the same allele, leaving genetic evidence about 11 individuals from 9 families (Figure 1).

Written informed consent was obtained from all individuals investigated or their guardians, and the ethics committee of the Technische Universität München approved the study.

Individual #49665 (family F1, Figure 1A) is a boy born to consanguineous parents from the UAE. He presented at the age of 10 years with mild intellectual disability, fatigability, mild hypertrophic cardiomyopathy, and visual impairment. At presentation he measured 134 cm with a body weight of 25 kg. Clinical examination revealed slight dyspnea when climbing stairs and mild intellectual disability. Plasma lactate was consistently elevated (3.0 to 7.2 mmol/l, reference < 2.1 mmol/l). Electroencephalogram, hearing test, and visual-evoked potentials showed no abnormalities. Electrocardiography (ECG) revealed signs of left ventricular hypertrophy confirmed by echocardiography. There was no obstruction of the left ventricular outflow tract. He had a pale optic disc on both sides but visual acuity and visual field could not be examined. Brain MRI was normal, but MR spectroscopy revealed lactate peaks in the parietal and precentral cortex. Respiratory chain (RC) measurement in muscle revealed a significant reduction of complex I and IV activities. He was substituted with CoQ_{10} (200 mg/day), riboflavin (400 mg/day), carnitine (1 g/day), and a fat-rich diet (60% of daily caloric intake). A follow-up examination 1 year after the initial presentation showed no significant changes of his clinical signs/symptoms.

His 17-year-old elder brother, individual #36349 (family F1, Figure 1A), had a very similar clinical picture.

Individual #66143 (family F2, Figure 1A), a boy, is the second child of healthy unrelated parents of Arab-Moslem origin from Israel. He presented at the age of 2 years with sudden respiratory failure. Heart ultrasonography indicated a hypertrophic cardiomyopathy and congestive heart failure. His cardiac symptoms improved on treatment with furosemide, spironolactone, carvedilole, and digoxin. In addition, a high-dose vitamin treatment (100 mg/day riboflavin, 100 mg/day vitamin B1, and 60 mg/day CoQ_{10}) was initiated. RC enzyme measurement in muscle revealed a significant reduction of complex I and IV activities. On follow-up examinations (over 3 years), the child's psychomotor development is normal and his parents reported that he is active like his peers. Digoxin and spironolacton treatment was stopped and his recent echocardiography revealed a stable condition of the heart including normal global function of left ventricle with no further hypertrophy of interventricular septum and no pulmonary hypertension.

Individual #72425 (family F3, Figure 1A) was a girl born to unrelated parents. At 3 months of age, she had feeding difficulties and failure to thrive. At the age of 7 months,

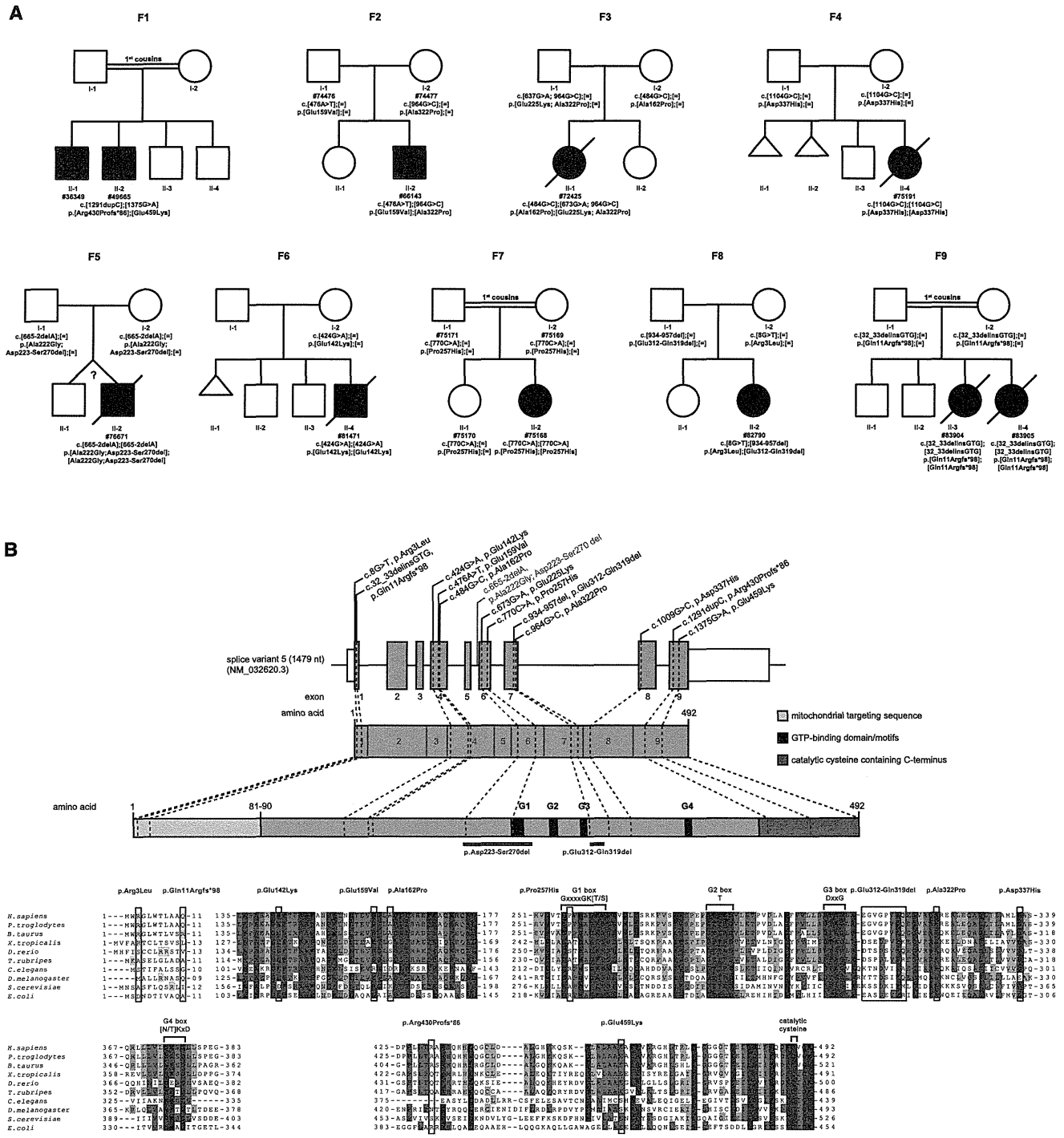

Figure 1. *GTPBP3* Mutation Status and Gene Structure
(A) Pedigrees of nine families with mutations in *GTPBP3*.
(B) Gene structure of *GTPBP3* with known protein domains of the gene product and localization and conservation of amino acid residues affected by mutations. Black and orange text indicate exonic and intronic variants. Intronic regions are not drawn to scale. Coloring in the sequence alignment represents the identity of amino acid residues.

she developed recurrent cough and fever and was admitted to the emergency room with severe fatigue, pallor, and progressive malaise. Blood exams showed leukocytosis, and 2 days later her general condition worsened, showing cyanosis and hyporeactivity. Echocardiography showed severe dilated cardiomyopathy with an ejection fraction of 20% that was unresponsive to therapy. She had severe refractory hyperlactatemia (23.3 mmol/l, reference range 0.5–2.3 mmol/l). Histochemical and spectrophotometric analysis of the muscle biopsy showed a severe complex IV deficiency. She died 10 days after admission from cardiac failure.

Individual #75191 (family F4, Figure 1A), a girl, was born to nonconsanguineous parents after an uneventful pregnancy of 40 weeks. The mother had had two miscarriages at 6 and 8 weeks and had a healthy son aged 16 months. In the first hours after birth, individual #75191 developed mild stridor and dyspnea which rapidly worsened. She fed poorly and became less responsive, and a Kussmaul breathing pattern was seen. She was transferred to a specialist center and was found to be severely hypotonic, moving very little, either spontaneously or after stimulation. She had hyperlactatemia (23 mmol/l), hypoglycemia (18 mg/dl), hyperammonemia (135 μmol/l, control value 11–48 μmol/l), and hyperlactaturia. She progressively developed respiratory insufficiency and bradycardia. Cardiac ultrasound showed apical right ventricular hypertrophy and an open duct of Botalli with minor shunting. Fractional shortening was 28% (mildly decreased). Cerebral ultrasound showed a minimal grade I bleeding, and the cerebral matter appeared mildly hyperechogenic. She died of asystolia at day 1. A muscle biopsy performed immediately after death showed decreased activities of RC complexes I and IV.

Individual #76671 (family F5, Figure 1A) was the second boy of nonconsanguineous parents. The infant was born at 41 weeks of gestation from a twin pregnancy. Generalized hypotonia and difficulty in suction was noted since birth and he rapidly developed failure to thrive. He acquired head control at the age of 7 months but parents reported normal cognitive skills. At the age of 9 months he was admitted to the intensive care unit for acute aspiration pneumonia that required intubation. Laboratory test revealed a metabolic acidosis with hyperlactatemia (5.2 mmol/l) and brain MRI showed bilateral thalamic T2-weighted hyperintense abnormalities with low diffusion. Analysis of a muscle biopsy revaled a clear reduction in histochemical cytochrome *c* oxidase activity and decreased complex I and IV enzyme activities. The cardiological examination disclosed hypertrophic cardiomyopathy and a Wolff-Parkinson-White pre-excitation syndrome (MIM 194200). The baby died after 15 days of hospitalization with clinical signs of heart failure.

Individual #81471 (family F6, Figure 1A) was a boy born to nonconsanguineous Romanian parents at 34 weeks gestation (birth weight 2.18 kg). His mother had premature and prolonged (85 hr) rupture of membranes before delivery, and the baby was treated with i.v. antibiotics before being discharged home on day 7. He was readmitted to hospital on day 25 with weight loss (2.23 kg). He was hypothermic and jaundiced and initial blood analysis showed profound metabolic acidosis. He was treated with i.v. antibiotics for presumed sepsis. The acidosis did not resolve, and serum lactate was elevated (11.0 mmol/l). ECG was abnormal and echocardiography showed concentric left ventricular hypertrophy. CSF lactate was 12.4 mmol/l (normal range 0.9–2.4 mmol/l) prompting bicarbonate treatment. Brain MRI showed abnormal diffusion of the subthalamic nuclei extending down to the brain stem. There was abnormal T2 signal in the midbrain and basal ganglia bilaterally. On examination he was thin but not dysmorphic. He was mildly jaundiced and had puffy feet. There was little spontaneous movement but normal muscle bulk and he was distinctly hypotonic. Feeding through a nasogastric tube was established but he did not become responsive despite high caloric intake. He developed recurrent apnea and died aged 5 weeks. Biochemical analysis performed in muscle revealed a significant decrease of RC complexes I and IV.

Individual #75168 (family F7, Figure 1A) is the second girl of first-cousin parents from India. She was first seen at the age of 2 years with development delay. She was able to walk but she couldn't speak. She received occupational and speech therapy. During a febrile illness when she was 3 years old, she had an acute metabolic failure with hyperlactatemia and hyperlactatorachia. She recovered but had epileptic seizures and more severe intellectual disability. Brain MRI showed pronounced bilateral hyperintensities affecting the whole thalamus and extending to the mesencephalon. Hyperlactatemia (>10 mmol/l) and hyperlactatorachia (6 mmol/l) were noticed. RC activity in muscle was normal as well as PDH complex tested by immunoblot. The girl was treated with qa carnitine 3 × 350 mg/day, CoQ_{10} 3 × 50 mg/day, vitamins B1 3 × 50 mg/day and B6 3 × 50 mg/day, and bicarbonate 4 × 1 g. Epilepsy was in good control with levetiracetame 40 mg/kg/day and a high-fat diet. The girl is in a special school for children with developmental delay. Her general condition is good. She is always in a good temper. Development is delayed about 1.5 years. She has continual hyperlactatemia (8–10 mmol/l).

Individual #82790 (family F8, Figure 1A) is a girl born at 40 weeks of gestation with normal birth weight to nonconsanguineous Japanese parents. At the age of 1 year, she developed frequent epileptic seizures, and she was medicated with phenobarbital. Severe developmental delay was noted and at the age of 15 months she was admitted to children's hospital. Her weight gain (9.25 kg, −0.06 SD) is within the normal range, but she developed severe muscle hypotonia. There is no cardiac involvement by ECG and echocardiogram. Hyperlactatemia was noted (5.72–6.49 mmol/l) whereas metabolic profiling of amino acids, urinary organic acids, and acylcarnitine was normal. RC analysis in muscle showed a significant decrease in complexes I and IV activities. Brain MRI showed bilateral hyperintensities in the putamen and weakly also in the anterior thalamus. A lactate peak was detected on $[H^+]$-MR spectroscopy. She is now 2 years of age and still presents with a severe global developmental delay.

Individual #83904 (family F9, Figure 1A) was the second child of consanguineous, healthy parents of Turkish origin. She was born at 39 weeks of gestational age (birth weight 2,740 g, length 49 cm, head circumference 32 cm). Shortly after birth, she presented with Wolff-Parkinson-White syndrome. Cardiac ultrasound was normal. Treatment was started with amiodarone and she

Table 1. Genetic and Clinical Findings in Individuals with *GTPBP3* Mutations

		***GTPBP3* Mutations**	**OXPHOS Activities in Skeletal Muscle**				**Clinical Features**				
ID	**Sex**	**cDNA (NM_032620.3) and Protein (NP_116009.2)**	**RCC**	**% of Lower Control Range**	**Absolute Values**	**Reference Range**	**AO**	**Course**	**HCM**	**Histochemical COX Defect**	**Other Features**
#49665[a,b]	male	c.[1291dupC; 1375G>A], p.[Pro430Argfs*86; Glu459Lys]	I	15%	0.025	0.17–0.56	10 years	alive 14 years	yes	ND	consanguineous parents (1st cousins), mild intellectual disability, fatigability, limited vision, lactic acidosis
			II	ND	ND	ND					
			II+III	normal	0.201	0.08–0.48					
			IV	24%	0.267	1.1–5.0					
#36349[b]	male	c.[1291dupC; 1375G>A], p.[Pro430Argfs*86; Glu459Lys]	I	no data	no data	no data	no data	alive 17 years	no data	no data	sibling of #49665 with similar clinical symptoms
			II								
			II+III								
			IV								
#66143[a]	male	c.[476A>T; 964G>C], p.[Glu159Val; Ala322Pro]	I	7%	0.01	0.19–0.48	2 years	alive 5 y ears	yes	ND	unrelated parents, sudden respiratory failure, lactic acidosis
			II	normal	0.10	0.07–0.12					
			II+III	normal	0.12	0.09–0.22					
			IV	28%	0.12	0.44–0.92					
#72425[a]	female	c.[484G>C; 673G>A; 964G>C], p.[Ala162Pro; Glu225Lys; Ala322Pro]	I	14%	0.015	0.11–0.30	3.5 months	died 8 months	DCM	yes	unrelated parents, cyanosis, hyporeactivity, DCM with residual ejection fraction of 20%, lactic acidosis
			II	normal	0.21	0.12–0.25					
			II+III	normal	0.06	0.006–0.14					
			IV	45%	0.76	1.7–4.0					
#75191[a]	female	c.[1009G>C; 1009G>C], p.[Asp337His; Asp337His]	I	31%	0.03	0.10–0.25	birth	died 1 day	yes	yes	unrelated parents, Kussmaul breathing, stridor, hypotonic, hyporeactivity, RVH, lactid acidosis
			II	normal	0.16	0.14–0.25					
			II+III	normal	0.12	0.13–0.25					
			IV	15%	0.09	0.60–1.48					
#76671	male	c.[665−2delA; 665−2delA], p.[Ala222Gly; Asp223_Ser270del; Ala222Gly; Asp223_Ser270del]	I	45%	0.05	0.11–0.30	birth	died 10 months	yes	yes	unrelated parents, hypotonia from birth, RVH, WPW, lactic acidosis
			II	normal	0.16	0.12–0.25					
			II+III	ND	ND	0.06–0.14					
			IV	17%	0.29	1.7–4.0					
#81471[a]	male	c.[424G>A; 424G>A], p.[Glu142Lys; Glu142Lys]	I	12%	0.012	0.104 ± 0.036	4 weeks	died 5 weeks	yes	yes	consanguineous parents, two healthy siblings, one miscarriage, FTT, poor weight gain and feeding, concentric LVH, lactic acidosis
			II	normal	0.098	0.145 ± 0.047					
			II+III	normal	0.850	0.544 ± 0.345					
			IV	17%	0.127	1.124 ± 0.511					

(*Continued on next page*)

Table 1. ***Continued***

		***GTPBP3* Mutations**	**OXPHOS Activities in Skeletal Muscle**				**Clinical Features**				
ID	**Sex**	**cDNA (NM_032620.3) and Protein (NP_116009.2)**	**RCC**	**% of Lower Control Range**	**Absolute Values**	**Reference Range**	**AO**	**Course**	**HCM**	**Histochemical COX Defect**	**Other Features**
#75168[a]	female	c.[770C>A; 770C>A], p.[Pro257His; Pro257His]	I	normal	no data	no data	2 years	alive 5 years	no	ND	consanguineous parents (1st cousins), developmental delay, epileptic seizures, intellectual disability, MRI hyperintense lesions of basal ganglia typical to Leigh syndrome, lactic acidosis
			II	normal							
			II+III	normal							
			IV	normal							
#82790[a]	female	c.[8G>T; 934_957del], p.[Arg3Leu; Gly312_Val319del]	I	36%	0.107	0.301 ± 0.05	1 year	alive 2 years	no	ND	unrelated parents, seizures, severe hypotonia, developmental delay, lactic acidosis
			II	normal	0.424	0.272 ± 0.05					
			II+III	normal	0.21	0.25 ± 0.093					
			IV	21%	0.008	0.035 ± 0.011					
#83904[a,c]	female	c.[32_33delinsGTG; 32_33delinsGTG], p.[Gln11Argfs*98; Gln11Argfs*98]	I	64%	4.2	6.5–17	1 week	died 9 months	yes	ND	consanguineous parents (1st cousins), lactic acidosis, WPW
			II	normal	16.1	13.6–45.7					
			II+III	normal	5.8	4.3–13.2					
			IV	25%	9.9	74–294					
#83905[a,c]	female	c.[32_33delinsGTG; 32_33delinsGTG], p.[Gln11Argfs*98; Gln11Argfs*98]	I	no data	no data	no data	birth	died 10 days	yes	ND	consanguineous parents (1st cousins), lactic acidosis, WPW
			II								
			II+III								
			IV								
#66654[a]	female	c.[673G>A; 964G>A]; [=] p.[Glu255Lys; Ala322Pro]; [=]	I	64%	0.09	0.14–0.35	1.5 months	alive	no	ND	intrauterine growth retardation, lactic acidosis, leukodystrophy, generalized hypotonia
			II	normal	0.19	0.18–0.41					
			II+III	90%	0.27	0.30–0.67					
			IV	normal	1.42	0.42–1.26					

Abbreviations are as follows: AO, age of onset; HCM, hypertrophic cardiomyopathy; DCM, dilated cardiomyopathy; FTT, failure to thrive; LVH/RVH, left/right ventricular hypertrophy; ND, not determined; WPW, Wolff-Parkinson-White syndrome.
Mitochondrial respiratory chain complexes (RCC) in muscle: I, NADH:CoQ-oxidoreductase; II, succinate:CoQ-oxidoreductase; II+III, succinate:cytochrome c reductase; IV, cytochrome c oxidase (COX).
Enzyme activities were determined in muscle biopsies and normalized to citrate synthase (CS). Absolute values and reference ranges are given in [mU / mU CS].
[a]Investigated by exome sequencing.
[b,c]These individuals are siblings.

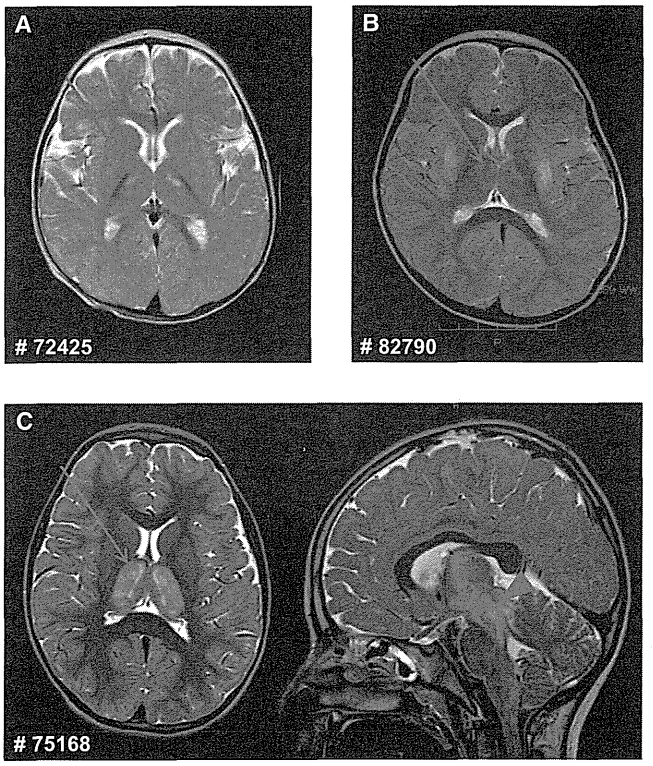

Figure 2. Brain MRI of Affected Individuals #72425, #82790, and #75168

(A) MRI of individual #72425 shows small T2 hyperintensities in the anterior thalamus bilaterally (arrow).

(B) In individual #82790, T2-weighted MRI shows bilateral hyperintensities in the putamen (arrowhead) and weakly also in the anterior thalamus (arrow).

(C) T2-weighted MRI of individual #75168 shows pronounced bilateral hyperintensities affecting the whole thalamus (arrow, axial view at the left) and extending to the mesencephalon (arrowhead, sagittal view at the right).

remained stable, without cardiac symptoms or arrhythmia. At 7 months of age, she had cardiogenic shock and metabolic acidosis. Heart ultrasound detected dilated cardiomyopathy and decreased contractility (ejection fraction 35%). She presented hyperlactatemia (20 mmol/l), hyperalaninemia (1,175 μmol/l; normal range, 190–450 μmol/l), and an increased lactate-to-pyruvate ratio (47; normal range, 10–20). Her disorder progressed despite intensive medication for heart failure. She died at the age of 9 months of cardiac insufficiency with arrhythmia.

Her younger sister, individual #83905 (family F9, Figure 1A), had a very similar clinical picture. She died at 6 months of age of cardiac insufficiency unresponsive to resuscitation procedures.

Genetic, biochemical, and clinical findings are summarized in Table 1. Pedigrees of the families we studied are shown in Figure 1A. The location of the identified mutations within the gene and the conservation of the affected amino acid (aa) residues are shown in Figure 1B. Individual #49665 (F1: II-2) was found to carry a frame shift and one missense variant. The next generation sequencing (NGS) data demonstrated a compound heterozygous status of the two variants (Figure S1 available online). Individual #76671 (F5: II-2) was homozygous for an intronic single base pair deletion, c.665−2delA, which is predicted to cause the loss of a splice acceptor site. Analysis of cDNA from fibroblasts revealed a shorter transcript, and sequencing found that in more than 95% of transcripts, the downstream acceptor of exon 7 was used for splicing, resulting in the skipping of exon 6 including the conserved G1-box guanine nucleotide-binding signature motif (Figure S2). Individual #82790 (F8: II-2) was found to be compound heterozygous for a missense mutation c.8G>T (p.Arg3Leu) and a 24 bp deletion c.934_957del (p.Gly312_Val319del). The 24 bp deletion is predicted to cause the deletion of 8 amino acids containing conserved residues. The p.Arg3Leu substitution at the very N terminus of the protein is scored as a predicted polymorphism but causes a loss of a positively charged residue, which is predicted to interfere with mitochondrial targeting (Predotar, PsortII). The two missense variants found in individual #66654, c.[673G>A; 964G>C], p.[Glu225Lys; Ala322Pro], were identical to the variants found on the paternal allele of individual #72425 (F3: II-1). Analysis of parental DNA revealed that both variants were also located on the same allele in individual #66654, meaning that only one allele is affected. Because of this observation, combined with the absence of a heart phenotype and because this individual is the only one exhibiting an isolated complex I defect, we consider the mutations found in *GTPBP3* not to be causative in subject #66654.

In summary, the identification of 13 different alleles in 11 individuals with suspected mitochondrial disease from 9 families provides strong evidence for the pathological role of mutant *GTPBP3* in the investigated families. It links *GTPBP3* mutations to combined respiratory chain complex deficiency (9/11), cardiomyopathy (9/11), lactic acidosis (11/11), and encephalopathy (4/11).

Brain MRI was performed in three individuals (Figure 2). It showed bilateral T2 hyperintensities in the thalamus, ranging from weak (#82790) or small (#72425) changes in the anterior thalamus to very pronounced hyperintensities affecting the whole thalamus in individual #75168. In addition, T2 hyperintensities affected the putamen bilaterally in individual #82790 and extended markedly to the mesencephalon in individual #75168. Taken together, the MRI involvement of basal ganglia and brainstem resembles the (MRI) findings in Leigh syndrome (which is, however, an ill-defined entity).

Skin fibroblast cell lines were available from seven individuals for functional studies. We first analyzed the cellular oxygen consumption rate (OCR[13]) by microscale respirometry with the XF96 extracellular flux analyzer (Seahorse Bioscience). When cells of individuals from families F1 to F5 were cultured in glucose-containing medium, only cell lines from individuals #75191 (F4: II-4) and #76671 (F5: II-2) showed a decreased OCR (of 59% and 58%, respectively) indicating defective oxidative phosphorylation

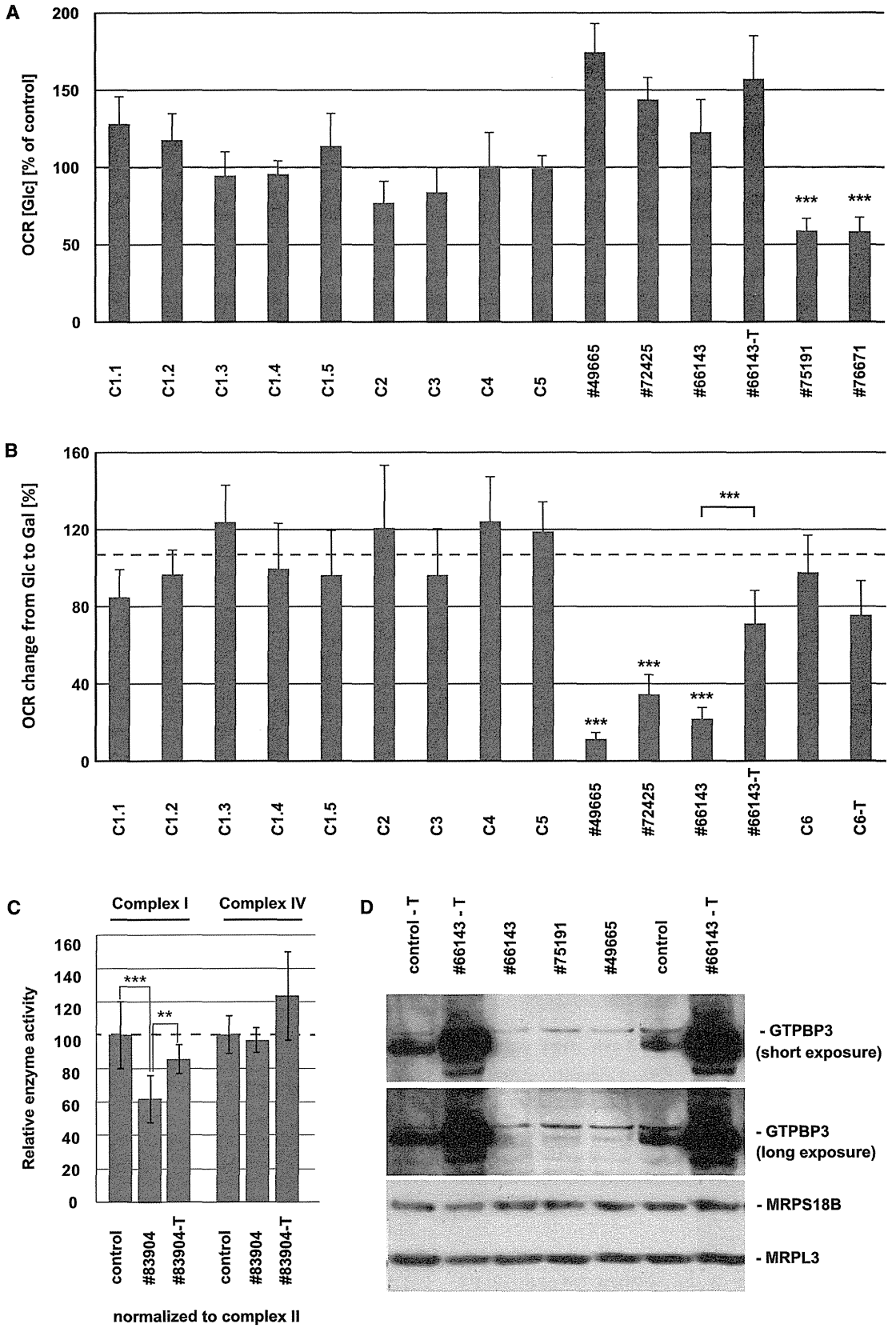

Figure 3. Analysis of Respiration Defects and GTPBP3 Protein Levels in Fibroblast Cell Lines

(A) Oxygen consumption rate (OCR) of fibroblast cell lines from five affected individuals and five control subjects cultured in high-glucose (Glc) medium. Each analysis was performed in more than 15 replicates. Control one (C1) was measured five time at different passage numbers (C1.1–1.5, NHDFneo, Lonza). OCR was expressed as percentage relative to the average of all controls. Cells from

(legend continued on next page)

(Figure 3A). When cells were cultured with galactose as the primary carbon source, rather than glucose, cells are forced to rely on oxidative phosphorylation rather than glycolysis in order to meet the energy demand.[14,15] Accordingly, in control cells an increase in OCR of approximately 2-fold was observed when galactose was substituted as the primary carbon source. This increase in OCR was impaired in fibroblasts from affected individuals #49665 (F1: II-2), #66143 (F2: II-2), and #72425 (F3: II-1), which showed OCR increases of only 11%, 35%, and 22%, respectively (Figure 3B). In order to confirm that defects in GTPBP3 are the cause of this defect, we transduced three cell lines with a wild-type copy of *GTPBP3* cDNA (RefSeq NM_32620.3) by using a lentiviral vector (pLenti 6.3/V5 TOPO, Life Technologies) as previously described.[16,17] Fibroblasts from individuals #49665 and #66143 were used for the rescue experiment, with fibroblasts from #66654 (subject with only one affected allele) being included as a control (C6). Unfortunately, we were unable to recover any viable cells from subject #49665 after the transduction procedure. Although the transduction had no noticeable effect on the control cell line (C6-T), transduced fibroblasts from #66143 (#66143-T) displayed a significant improvement of OCR in galactose-containing medium (Figure 3B). Furthermore, we detected an isolated respiratory chain complex (RCC) I deficiency in a fibroblast cell line from family 9. Cotransfection of individual #83904 fibroblasts with two putative *GTPBP3* isoforms amplified by RT-PCR, RefSeq NM_32620.3 and NM_0128855.2 (missing 63 base pairs of exon 8), significantly improved enzyme activities of RCC I (pIRES2-EGFP, Clontech) (Figure 3C). Analysis of the protein levels of GTPBP3 in five fibroblast cell lines demonstrated reduced or undetectable amounts in individuals #49665, #75191, #66143, #83904, and #83905, although they showed a clear increase after transduction or transfection (Figures S4 and 3D). In conclusion, our data demonstrate a causal role for *GTPBP3* mutations in the oxidative metabolism deficiency in these individuals.

Given that homologs of GTPBP3 in other systems have been implicated in protein synthesis, we next concentrated on the analysis of GTPBP3 in mitochondrial translation. The synthesis of mtDNA-encoded polypeptides, investigated by pulse-labeling of mitochondrial translation products via [^{35}S]methionine in fibroblasts of affected individuals (for methods see Haack et al.[18]) was severely and uniformly decreased to 20%–30% of control levels in individuals #49665, #66143, and #75191 (Figures 4A and 4B). There was no detectable defect in fibroblasts from individual #72425, which might be explained by the relatively low conservation of the mutated residue in this individual (Figure 1B). In order to exclude possible defects of mitochondrial transcription or precursor RNA processing, we analyzed all mitochondrially encoded rRNAs and mRNAs in fibroblasts of individuals #49665, #66143, #72425, and #75191 by RNA blotting and by RNA-seq in fibroblasts of individual #49665. We found no differences in the expression levels of the mt-RNAs between case and control subjects. On average, the mt-RNA expression levels were only 6% lower in individual #49665 as compared to control individuals (data not shown). We did not observe any appreciable reduction in steady-state levels of mature RNAs, nor was there any accumulation of precursor RNAs (Figure S3A). Next, we analyzed the steady-state levels of mt-tRNAs, including those five species for which the τm^5 U modification has been reported in mammals (Gln, Glu, Lys, Leu^{UUR}, and Trp).[4] We again observed no appreciable changes in their steady-state levels (Figure S3B). In order to further corroborate a direct role of GTPBP3 in mitochondrial translation, we downregulated its expression via RNA interference in HeLa cells (Figure 4C). Reduction of GTPBP3 protein levels upon RNAi treatment of HeLa cells was comparable to the reduction of its level in *GTPBP3* mutant fibroblasts (Figure 4D). Downregulation of *GTPBP3* expression resulted in a general mitochondrial translation defect, similarly to the reduction observed in subject fibroblasts (Figure 4D). In conclusion, the reduced translation efficiency observed in three out of four *GTPBP3* mutant cell lines, as well as in human cells treated with *GTPBP3* RNAi, confirmed an important function for GTPBP3 in efficient mitochondrial protein synthesis.

In order to test the consequences of this reduced translation rate upon the protein levels of OXPHOS complexes in mutant fibroblast cell lines, we analyzed the steady-state levels of several nuclear-encoded subunits of the OXPHOS system by immunoblotting. In fibroblasts from individuals #72425, #75191, and #76671 (F3: II-1, F4: II-4, and F5: II-2), we observed strongly reduced amounts of RCC IV. Fibroblasts from subjects #72425, #75191, and #49665 also showed reduced levels of RCC I, whereas the levels

individuals #75191 and #76671 showed a significant reduction of oxygen consumption whereas cells from individuals #49665, #72425, and #66143 presented no defective respiration. Error bar indicates 1 SD; ***$p < 0.001$.

(B) Oxygen consumption rate of fibroblast cells cultured in galactose (Gal) growth medium. The average increase of OCR from five control cells cultured in galactose-containing medium compared to glucose-containing medium was 107%. Cell lines from individuals #49665, #72425, and #66143 show significant lower increase in OCR. Lentiviral expression of wt*GTPBP3* in cells from individual #66143 significantly increases the change in OCR although it has only little effect in control cells (C6-T). Error bar indicates 1 SD; ***$p < 0.001$.

(C) Activities of respiratory chain complexes I and IV (expressed as ratio to CII activity) are decreased in individual #83904 cells transfected by electroporation with empty vector (pIRES2-EGFP) according to the manufacturer's protocol (LONZA) but are improved upon expression of *GTPBP3* cDNAs from the same plasmid. Measurements were performed as previously described.[29,30] Error bar indicates 1 SD. Activity in controls was set as 100%. **$p < 0.01$, **$p < 0.001$.

(D) Levels of GTPBP3 were reduced in cells from individuals #49665, #75191, and #66143 and elevated after transduction with wt*GTPBP3* cDNA. MRPS18B and MRPL3 served as mitochondrial loading controls.

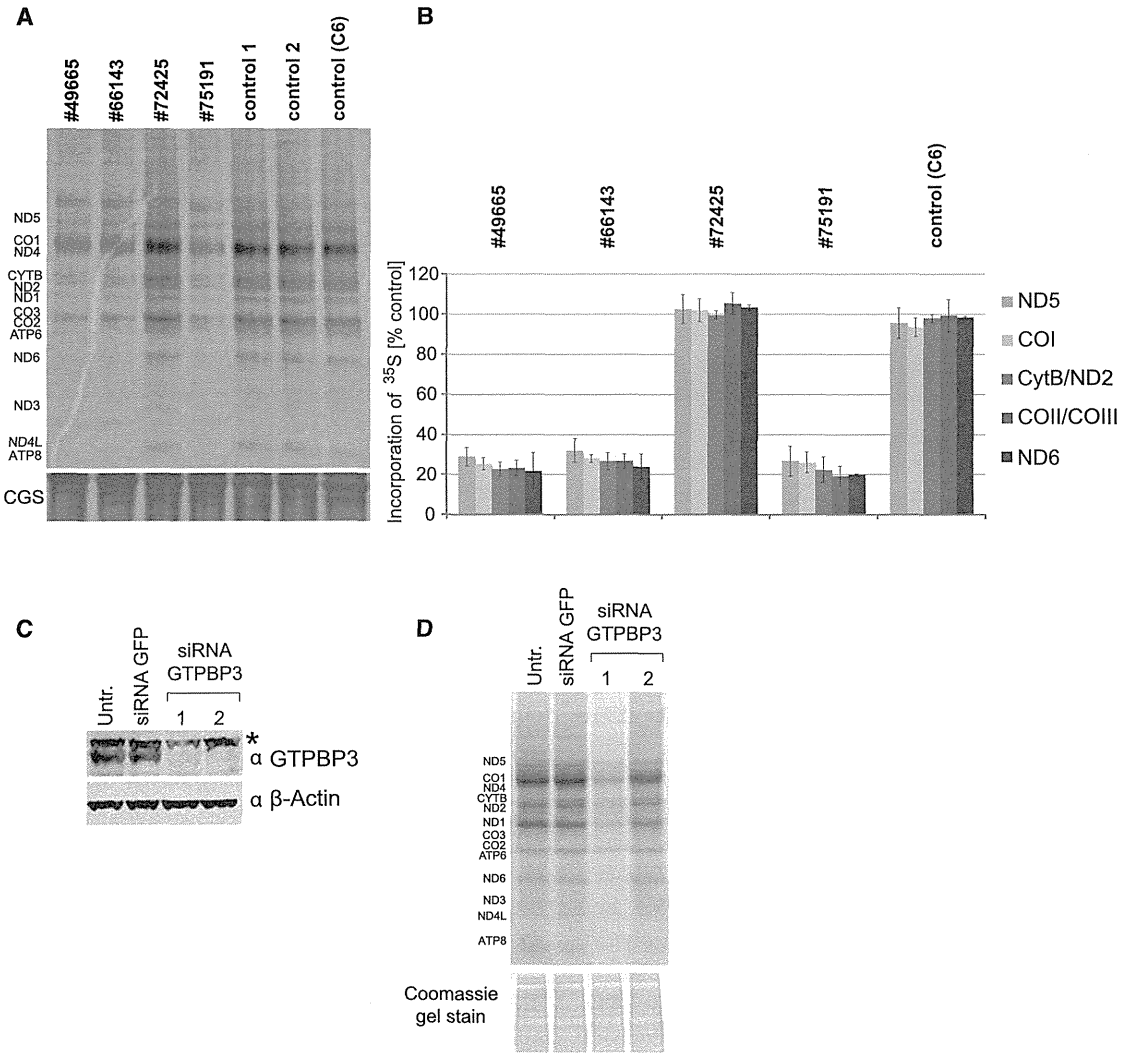

Figure 4. Analysis of Mitochondrial Protein Synthesis in Primary Fibroblasts and in HeLa Cells Treated with RNAi against GTPBP3
(A) [^{35}S]methionine metabolic labeling of mitochondrial proteins in fibroblasts. Products of mitochondrial translation were labeled with [^{35}S]methionine for 30 min, separated by a 4%–12% gradient SDS-PAGE, and visualized by autoradiography. To validate equal protein loading, a small section of the gel was stained with Coomassie (CGS). Fibroblasts from individuals #49665, #66143, and #75191 demonstrate significant inhibition of mitochondrial protein synthesis although translation in cells from individual #72425 is not affected.
(B) Quantification of radiolabelled products of mitochondrial translation. Incorporation of [^{35}S] as in (A) was quantified by ImageQuant software after exposure to a PhosphorImager screen from three independent experiments. Error bar indicates 1 SD.
(C) Downregulation of GTPBP3 in HeLa cells via RNA interference. Immunoblot analysis of total HeLa cell lysate transfected with two different siRNA to GTPBP3 show decreased level of GTPBP3 upon RNAi treatment for 6 days. siRNA to GFP was used as transfection control. Asterisk indicates nonspecific band recognized by anti-GTPBP3 antibody in HeLa cells. β-actin serves as a loading control. Two different siRNA duplexes targeting GTPBP3 were used, 1 and 2.
(D) Mitochondrial translation in HeLa cells upon GTPBP3 downregulation. HeLa cells were transfected for 6 days with siRNA against GTPBP3 and subjected to [^{35}S]methionine metabolic labeling. Inactivation of GTPBP3 leads to the reduced efficiency of mitochondrial translation. Two different siRNA duplexes targeting GTPBP3 were used, 1 and 2.

of RCC II and V remained normal in all cell lines (Figure 5). The diminished steady-state levels of respiratory chain complexes I and IV in fibroblast cell lines are in agreement with the impaired mitochondrial de novo translation rates in these cells and match the enzymatic defects identified in muscle biopsies of the same individuals.

Within an international cooperation between European (Germany, UK, Italy, France, and Belgium), Israeli, and Japanese Centers for mitochondrial disorders, we provide statistically convincing evidence for *GTPBP3* mutations leading to mitochondrial disease. To further support collaborative studies, the global mitochondrial disease community has established a Mitochondrial Disease Sequence Data Resource (MSeqDR) for common genomic data deposition and mining.

The genotype-driven analysis performed here was independent from the clinical presentation. Nevertheless, we identified common clinical features of the affected individuals that include lactic acidosis (11/11), cardiomyopathy (9/11), and neurological symptoms (6/11). The latter

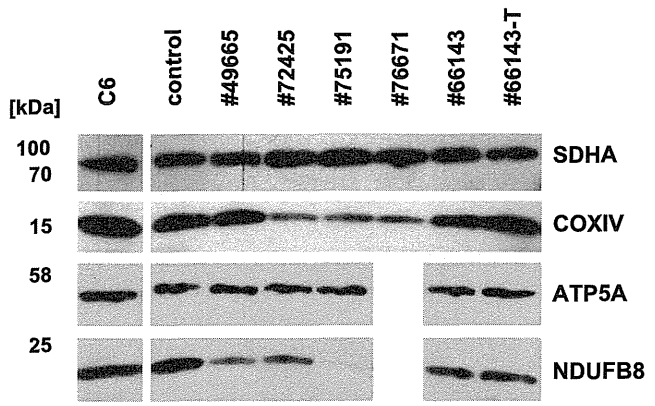

Figure 5. Immunoblot Analysis of OXPHOS Proteins in Fibroblasts

10 μg of detergent-solubilized total cell extract was subjected to immunoblot analysis of OXPHOS components. Amounts of SDHA (complex II) and ATP5A (ATPase) were unchanged in all individuals. In cells from individuals #72425, #75191, and #76671, a reduction of COXIV (complex IV) was observed. Cells from individuals #49665, #72425, and #75191 showed decreased levels of NDUFB8 (complex I). Antibodies used: mouse antibodies against SDHA (ab14715), NDUFB8 (ab110242), ATP5A (ab14748), and rabbit antibodies against COXIV (ab16056) from Abcam and rabbit anti GTPBP3 (HPA042158) from SIGMA Aldrich.

comprised symptoms such as development delay, intellectual disability, feeding difficulties, muscle hypotonia, fatigue, visual impairment, and epileptic seizures. Severity of the disease ranged from neonatal onset and death to late-infantile onset and survival into the second decade of life. Most affected individuals, however, manifested clinical symptoms before their first birthday. This is consistent with the normal cellular respiration, in organello translation, and normal levels of respiratory chain complexes reported in individuals less severely affected and the significantly reduced mitochondrial translation, respiration, and low levels of complex I and IV in those severely affected.

Modifications of the tRNA "wobble-base" in the anticodon loop are required for accurate and efficient codon recognition. The modification of position 5 (xm^5) of the U34 wobble-base of certain tRNAs is evolutionarily well conserved, although different modified side chains have been identified in different species. In mammals, mitochondria 5-taurinomethyluridine (τm^5U34) is found at the wobble-base position.[19] Based upon studies in bacteria and yeast mitochondria, GTPBP3 and MTO1 have been proposed to generate this modification in mammalian mitochondria. Although this prediction awaits direct biochemical validation, the proposed functional conservation of GTPBP3 and MTO1 has been supported by the mitochondrial localization of these proteins in human cells and by complementation of the respiratory-deficient phenotype in yeast by their mammalian homolog cDNAs.[20,21] Functional deficiency of homologs of GTPBP3 and MTO1 in bacteria and yeast mitochondria has been associated with abnormal U34 modification and consequently a reduced efficiency of translation.[21–23] Our data support an analogous activity of GTPBP3 in human mitochondria since we identified a reduced efficiency of translation in three cell lines with *GTPBP3* mutations and in cells with RNAi-mediated downregulation of GTPBP3 expression. Other groups have also reported impaired protein synthesis and reduced mitochondrial function in GTPBP3-depleted cells.[24] The defect in mitochondrial translation was a likely cause of the combined respiratory chain complex deficiency detected in muscle tissues of all but one affected individual.

Like *GTPBP3* mutations, *MTO1* mutations are also associated with hypertrophic cardiomyopathy (HCM), lactic acidosis, and combined respiratory chain deficiency. An association of *MTO1* mutations with impaired mitochondrial translation has yet to be shown for human mitochondria, but the common clinical presentation provides support for a common pathomechanism in the U34 modification for both diseases. So far, all individuals with *MTO1* mutations presented a HCM. However, nearly all of them have been specifically screened for *MTO1* mutations based on the clinical presentation of a HCM. Clinical and MRI signs of brain involvement are found for both *GTPBP3* and *MTO1* cases. The genotype-driven investigation presented here identified individuals with lactic acidosis, developmental delay, and MRI involvement of thalamus, putamen, and brainstem but without HCM. It can be expected that the clinical spectrum associated with MTO1 deficiency will also broaden, with more subjects being genome-wide investigated. In a very recent study, Taylor et al. indeed reported a case subject with *MTO1* mutations and central neurological features who did not have a cardiomyopathy.[25]

Our study highlights that defects in mitochondrial translation, probably owing to incorrect posttranscriptional modification of mt-tRNAs, are an important contributory factor to the spectrum of human mitochondrial disease. Recent data have suggested that more than 7% of all mt-tRNA residues undergo posttranscriptional modification, with close to 30 different modifications so far described.[4] Therefore, it is expected that future WES analyses of individuals clinically diagnosed with mitochondriopathy will reveal further mutations within genes coding for mt-tRNA modifiers. Indeed, in addition to the aforementioned mutations in *MTO1* and *TRMU*, mutations in *PUS1* (MIM 608109) (which introduces pseudouridine [Ψ] at base positions 27, 28, and 29 in several mt-tRNAs) have been reported in subjects affected with mitochondrial myopathy and sideroblastic anemia (MLASA)[26] (MIM 600462) and very recent studies have identified mutations in *TRIT1* (which is responsible for i^6A37 modification of a subset of mt-tRNAs) in individuals with severe combined mitochondrial respiratory chain defects.[27] Furthermore, mtDNA mutations in mt-tRNA genes, which are a very frequent cause of human respiratory chain deficiencies (MITOMAP), might also affect mt-tRNA modification. Related to the present study, it has been reported that τm^5U34 is not present in mt-tRNALeu^{UUR} harboring the m.3243A>G mutation (or other pathological mutations) responsible for mitochondrial encephalopathy, lactic

acidosis, and stroke-like episodes (MELAS) (MIM 540000). The absence of τm^5U34 has been suggested to be responsible for the mitochondrial translation defect in these subjects.[28] These results imply that deficiency of mt-tRNA modification plays a critical role in the molecular pathogenesis of human respiratory chain disease. Further studies of these pathways, such as analysis of tissue-specific regulation of mt-tRNA-modifying enzymes, might help to explain the clinical heterogeneity observed for mitochondrial diseases caused by mutations in mt-tRNA genes.

In conclusion, this study shows a mitochondrial translation disorder with a broad spectrum of clinical presentations, which emphasizes the importance of post-transcriptional modification of mitochondrial tRNAs for proper mitochondrial function.

Supplemental Data

Supplemental Data include four figures and can be found with this article online at http://dx.doi.org/10.1016/j.ajhg.2014.10.017.

Acknowledgments

We thank C. Terrile, M. Borzes, and C. Fischer for technical support and F. Miyake and T. Wada for referral of sample materials. This work was supported by the Deutsche Forschungsgemeinschaft within the framework of the Munich Cluster for Systems Neurology (EXC 1010 SyNergy), the German Bundesministerium für Bildung und Forschung (BMBF) through funding of the E-Rare project GENOMIT (01GM1207 for T.M. and H.P., 2011-RARE-005-03 for A.R. and M.D.M., J41J11000420001 for M.Z., and FWF I 920-B13 for J.A.M.), German Network for Mitochondrial Disorders (mitoNET 01GM1113C for T.M., H.P., and P.F. and 01GM1113A for T.K.), the German Center for Heart Research (Z76010017300 and Z56010015300 for T.M.), European Commission 7th Framework Program (Project N261123 GEUVADIS), Medical Research Council, UK (MC_U105697135 for T.J.N., J.R., S.F.P., C.A.P., and M.M.), Wellcome Trust Strategic Award (096919/Z/11/Z for R.W.T. and P.F.C.), MRC Centre for Neuromuscular Diseases (G0601943), UK NHS Highly Specialised "Rare Mitochondrial Disorders of Adults and Children" Service for R.W.T. and P.F.C., Fund for Scientific Research Belgium (FWO, contract number G.0200.10 for A.V., J.S., and R.V.C.), Fondazione Telethon (GGP11011 and GPP10005), Italian Ministry of Health (GR2010-2316392), CARIPLO (2011/0526), Pierfranco and Luisa Mariani Foundation, and Italian Association of Mitochondrial Disease Patients and Families (Mitocon) to D.G., F.I., E.L., and M.Z., Research Program of Innovative Cell Biology by Innovative Technology (Cell Innovation), Grant-in-Aid for the Development of New Technology from The Promotion and Mutual Aid Corporation for Private Schools of Japan from MEXT for Y.O., Grants-in-Aid for the Research on Intractable Diseases from the Ministry of Health, Labour and Welfare of Japan for A.O., Kawano Masanori Memorial Public Interest Incorporated Foundation for Promotion of Pediatrics for K. Murayama, Association Française contre les Myopathies (AFM) for A.R. and M.D.M., and Fellowship from the AFM (16615 for M.D.M.).

Received: July 30, 2014
Accepted: October 29, 2014
Published: November 26, 2014

Web Resources

The URLs for data presented herein are as follows:

MITOMAP, http://www.mitomap.org/MITOMAP
MSeqDR, https://mseqdr.org/
Online Mendelian Inheritance in Man (OMIM), http://www.omim.org/
Predotar, https://urgi.versailles.inra.fr/predotar/predotar.html
PSORTII Prediction, http://psort.hgc.jp/form2.html
RefSeq, http://www.ncbi.nlm.nih.gov/RefSeq

References

1. Boczonadi, V., and Horvath, R. (2014). Mitochondria: impaired mitochondrial translation in human disease. Int. J. Biochem. Cell Biol. *48*, 77–84.
2. Osawa, S. (1995). Evolution of the Genetic Code (Washington, DC: ASM Press).
3. Suzuki, T. (2005). Biosynthesis and function of tRNA wobble modifications. Top. Curr. Genet. *12*, 23–69.
4. Suzuki, T., and Suzuki, T. (2014). A complete landscape of post-transcriptional modifications in mammalian mitochondrial tRNAs. Nucleic Acids Res. *42*, 7346–7357.
5. Colby, G., Wu, M., and Tzagoloff, A. (1998). MTO1 codes for a mitochondrial protein required for respiration in paromomycin-resistant mutants of *Saccharomyces cerevisiae*. J. Biol. Chem. *273*, 27945–27952.
6. Yokoyama, S., Watanabe, T., Murao, K., Ishikura, H., Yamaizumi, Z., Nishimura, S., and Miyazawa, T. (1985). Molecular mechanism of codon recognition by tRNA species with modified uridine in the first position of the anticodon. Proc. Natl. Acad. Sci. USA *82*, 4905–4909.
7. Björk, G.R., Huang, B., Persson, O.P., and Byström, A.S. (2007). A conserved modified wobble nucleoside (mcm5s2U) in lysyl-tRNA is required for viability in yeast. RNA *13*, 1245–1255.
8. Yarham, J.W., Elson, J.L., Blakely, E.L., McFarland, R., and Taylor, R.W. (2010). Mitochondrial tRNA mutations and disease. Wiley Interdiscip. Rev. RNA *1*, 304–324.
9. Zeharia, A., Shaag, A., Pappo, O., Mager-Heckel, A.-M., Saada, A., Beinat, M., Karicheva, O., Mandel, H., Ofek, N., Segel, R., et al. (2009). Acute infantile liver failure due to mutations in the TRMU gene. Am. J. Hum. Genet. *85*, 401–407.
10. Ghezzi, D., Baruffini, E., Haack, T.B., Invernizzi, F., Melchionda, L., Dallabona, C., Strom, T.M., Parini, R., Burlina, A.B., Meitinger, T., et al. (2012). Mutations of the mitochondrial-tRNA modifier MTO1 cause hypertrophic cardiomyopathy and lactic acidosis. Am. J. Hum. Genet. *90*, 1079–1087.
11. Baruffini, E., Dallabona, C., Invernizzi, F., Yarham, J.W., Melchionda, L., Blakely, E.L., Lamantea, E., Donnini, C., Santra, S., Vijayaraghavan, S., et al. (2013). MTO1 mutations are associated with hypertrophic cardiomyopathy and lactic acidosis and cause respiratory chain deficiency in humans and yeast. Hum. Mutat. *34*, 1501–1509.
12. Elstner, M., Andreoli, C., Klopstock, T., Meitinger, T., and Prokisch, H. (2009). The mitochondrial proteome database: MitoP2. Methods Enzymol. *457*, 3–20.
13. Invernizzi, F., D'Amato, I., Jensen, P.B., Ravaglia, S., Zeviani, M., and Tiranti, V. (2012). Microscale oxygraphy reveals OXPHOS impairment in MRC mutant cells. Mitochondrion *12*, 328–335.
14. Petrova-Benedict, R., Buncic, J.R., Wallace, D.C., and Robinson, B.H. (1992). Selective killing of cells with oxidative

defects in galactose medium: a screening test for affected patient fibroblasts. J. Inherit. Metab. Dis. *15*, 943–944.
15. Robinson, B.H., Petrova-Benedict, R., Buncic, J.R., and Wallace, D.C. (1992). Nonviability of cells with oxidative defects in galactose medium: a screening test for affected patient fibroblasts. Biochem. Med. Metab. Biol. *48*, 122–126.
16. Danhauser, K., Iuso, A., Haack, T.B., Freisinger, P., Brockmann, K., Mayr, J.A., Meitinger, T., and Prokisch, H. (2011). Cellular rescue-assay aids verification of causative DNA-variants in mitochondrial complex I deficiency. Mol. Genet. Metab. *103*, 161–166.
17. Kornblum, C., Nicholls, T.J., Haack, T.B., Schöler, S., Peeva, V., Danhauser, K., Hallmann, K., Zsurka, G., Rorbach, J., Iuso, A., et al. (2013). Loss-of-function mutations in MGME1 impair mtDNA replication and cause multisystemic mitochondrial disease. Nat. Genet. *45*, 214–219.
18. Haack, T.B., Kopajtich, R., Freisinger, P., Wieland, T., Rorbach, J., Nicholls, T.J., Baruffini, E., Walther, A., Danhauser, K., Zimmermann, F.A., et al. (2013). ELAC2 mutations cause a mitochondrial RNA processing defect associated with hypertrophic cardiomyopathy. Am. J. Hum. Genet. *93*, 211–223.
19. Suzuki, T., Suzuki, T., Wada, T., Saigo, K., and Watanabe, K. (2002). Taurine as a constituent of mitochondrial tRNAs: new insights into the functions of taurine and human mitochondrial diseases. EMBO J. *21*, 6581–6589.
20. Li, X., and Guan, M.-X. (2002). A human mitochondrial GTP binding protein related to tRNA modification may modulate phenotypic expression of the deafness-associated mitochondrial 12S rRNA mutation. Mol. Cell. Biol. *22*, 7701–7711.
21. Li, X., Li, R., Lin, X., and Guan, M.-X. (2002). Isolation and characterization of the putative nuclear modifier gene MTO1 involved in the pathogenesis of deafness-associated mitochondrial 12 S rRNA A1555G mutation. J. Biol. Chem. *277*, 27256–27264.
22. Wang, X., Yan, Q., and Guan, M.-X. (2010). Combination of the loss of cmnm5U34 with the lack of s2U34 modifications of tRNALys, tRNAGlu, and tRNAGln altered mitochondrial biogenesis and respiration. J. Mol. Biol. *395*, 1038–1048.
23. Murphy, F.V., 4th, Ramakrishnan, V., Malkiewicz, A., and Agris, P.F. (2004). The role of modifications in codon discrimination by tRNA(Lys)UUU. Nat. Struct. Mol. Biol. *11*, 1186–1191.
24. Villarroya, M., Prado, S., Esteve, J.M., Soriano, M.A., Aguado, C., Pérez-Martínez, D., Martínez-Ferrandis, J.I., Yim, L., Victor, V.M., Cebolla, E., et al. (2008). Characterization of human GTPBP3, a GTP-binding protein involved in mitochondrial tRNA modification. Mol. Cell. Biol. *28*, 7514–7531.
25. Taylor, R.W., Pyle, A., Griffin, H., Blakely, E.L., Duff, J., He, L., Smertenko, T., Alston, C.L., Neeve, V.C., Best, A., et al. (2014). Use of whole-exome sequencing to determine the genetic basis of multiple mitochondrial respiratory chain complex deficiencies. JAMA *312*, 68–77.
26. Bykhovskaya, Y., Casas, K., Mengesha, E., Inbal, A., and Fischel-Ghodsian, N. (2004). Missense mutation in pseudouridine synthase 1 (PUS1) causes mitochondrial myopathy and sideroblastic anemia (MLASA). Am. J. Hum. Genet. *74*, 1303–1308.
27. Yarham, J.W., Lamichhane, T.N., Pyle, A., Mattijssen, S., Baruffini, E., Bruni, F., Donnini, C., Vassilev, A., He, L., Blakely, E.L., et al. (2014). Defective i6A37 modification of mitochondrial and cytosolic tRNAs results from pathogenic mutations in TRIT1 and its substrate tRNA. PLoS Genet. *10*, e1004424.
28. Yasukawa, T., Suzuki, T., Ueda, T., Ohta, S., and Watanabe, K. (2000). Modification defect at anticodon wobble nucleotide of mitochondrial tRNAs(Leu)(UUR) with pathogenic mutations of mitochondrial myopathy, encephalopathy, lactic acidosis, and stroke-like episodes. J. Biol. Chem. *275*, 4251–4257.
29. Rustin, P., Chretien, D., Bourgeron, T., Gérard, B., Rötig, A., Saudubray, J.M., and Munnich, A. (1994). Biochemical and molecular investigations in respiratory chain deficiencies. Clin. Chim. Acta *228*, 35–51.
30. Rustin, P., Chretien, D., Bourgeron, T., Wucher, A., Saudubray, J.M., Rotig, A., and Munnich, A. (1991). Assessment of the mitochondrial respiratory chain. Lancet *338*, 60.